

Neurochirurgische Klinik der Ludwig-Maximilians-Universität München

Direktor: Prof. Dr. med. Jörg-Christian Tonn



*Locoregional heterogeneity of glioblastoma entails pro- or antitumorigenic effects of tumor associated mesenchymal stem cells*

Dissertation

zum Erwerb des Doktorgrades der Medizin

an der Medizinischen Fakultät der

Ludwig-Maximilians-Universität München

vorgelegt von

Robin Waechter

aus

Gräfelfing

Jahr

2023

Mit Genehmigung der Medizinischen Fakultät der  
Ludwig-Maximilians-Universität zu München

Erster Gutachter: *Prof. Dr. rer. nat. Rainer Glaß*  
Zweiter Gutachter: *Prof. Dr. med Rainer Willy Hauck*  
Dritter Gutachter: *apl. Prof. Dr. med. Nathalie Albert*  
ggf. weitere Gutachter:

Mitbetreuung durch den  
promovierten Mitarbeiter:

Dekan: Prof. Dr. med. Thomas Gudermann

Tag der mündlichen Prüfung: 17.01.2023

## Table of content

<b>Zusammenfassung .....</b>	<b>5</b>
<b>Abstract.....</b>	<b>7</b>
<b>List of figures.....</b>	<b>8</b>
<b>List of abbreviations.....</b>	<b>9</b>
<b>1 Introduction.....</b>	<b>11</b>
1.1 <i>Glioblastoma multiforme</i> .....	11
1.1.1 Epidemiology and classification.....	11
1.1.2 Etiology .....	12
1.1.3 Histopathology.....	12
1.1.4 Pathogenesis.....	13
1.1.5 Diagnosis .....	15
1.1.6 Therapy.....	16
1.2 <i>Mesenchymal stem cells</i> .....	17
1.3 <i>Aim of thesis</i> .....	19
<b>2 Material and Methods.....</b>	<b>20</b>
2.1 <i>Material</i> .....	20
2.1.1 Devices & Softwares .....	20
2.1.2 In vitro: Cell culture .....	21
2.1.3 In vivo: Animal experiment.....	23
2.1.4 Histology.....	24
2.2 <i>Methods</i> .....	26
2.2.1 In vitro: Cell Culture .....	26
2.2.2 In vivo: Animal experiment.....	31
2.2.3 Histology.....	33
2.2.4 Microscopy .....	34
2.2.5 Statistical analysis .....	35
<b>3 Results .....</b>	<b>36</b>
3.1 <i>Mesenchymal stem cells migrate to invasive areas of the tumor</i> .....	36
3.2 <i>MSCs do not persist in the tumor core</i> .....	41
3.3 <i>Blood-brain barrier in GBM invasive areas appears largely intact</i> .....	43
3.4 <i>Serum-free MSCs conditioned medium increases viability of GSCs</i> .....	45

<b>4</b>	<b>Discussion.....</b>	<b>51</b>
4.1	<i>MSCs tropism for tumors .....</i>	<i>51</i>
4.2	<i>Importance of the tumor microenvironment.....</i>	<i>52</i>
4.3	<i>Pro- and antitumorigenic effects of MSC.....</i>	<i>54</i>
4.4	<i>Reciprocal interactions between MSCs and glioma cells.....</i>	<i>56</i>
4.5	<i>Perspective of MSC-based therapy for GBM .....</i>	<i>57</i>
<b>5</b>	<b>Conclusion .....</b>	<b>59</b>
	<b>List of references .....</b>	<b>60</b>
	<b>Acknowledgment.....</b>	<b>70</b>
	<b>Affidavit .....</b>	<b>71</b>
	<b>Lebenslauf .....</b>	<b>Fehler! Textmarke nicht definiert.</b>

# Zusammenfassung

Neben anderen Zelltypen des Tumorstromas, spielen mesenchymale Stammzellen eine wichtige Rolle im Progress des Glioblastoma multiforme. Bisher erhobene Daten zeigen kontroverse Resultate über die komplexen Interaktionsmechanismen zwischen mesenchymalen Stammzellen und Tumorzellen. Diese Studie analysiert das Migrationsverhalten von intrazerebral injizierter mesenchymaler Stammzellen. Weiterhin stellt ein *in vitro* Experiment einen pathologisch relevanten Aspekt der *in vivo* beobachteten Interaktion zwischen Glioblastomzellen und mesenchymalen Stammzellen nach, um einen die Viabilität der Tumorzellen beeinflussenden Effekt zu untersuchen.

Zunächst wurden Glioblastomzellen orthotop intrazerebral in Mäuse eingebracht. Sobald der Tumor eine ausreichende Größe erreicht hatte, wurden mesenchymale Stammzellen in den Tumor inokuliert. In darauffolgend angefertigten Gehirnschnitten untersuchte man die Migration der mesenchymalen Stammzellen und die Durchlässigkeit der Bluthirnschranke im Tumor. Weiterhin wurde die Viabilität von Glioblastomzellen in einem Proliferationsassay analysiert, nachdem diese mit einem serumfreien von mesenchymalen Stammzellen konditionierten Medium inkubiert worden sind. Der Grund hierfür liegt in der Annahme, dass mesenchymale Stammzellen eine wichtige Rolle in Wundheilungsprozessen nach Traumata einnehmen: Im akuten Stadium einer Verletzung koordinieren sie unter dem Einfluss von aus dem Blut stammenden Serumfaktoren Immunreaktionen, wohingegen sie später ohne den unmittelbaren Einfluss von Serumfaktoren, zur Wundheilung und Gewebsregeneration beitragen.

Das *in vivo* Experiment demonstriert die Migration der mesenchymalen Stammzellen hin zu den invasiven Bereichen des Tumors. In diesen zeigt sich die Bluthirnschranke weitestgehend intakt, sodass Serumfaktoren größer als 70 kDa diese nicht überwinden können. Folglich wurden die serumfreien Bedingungen, in denen sich mesenchymale Stammzellen im Glioblastom wiederfinden, in einem *in vitro* Versuch modelliert. Von mesenchymalen Stammzellen unter serumfreien Bedingungen konditioniertes Medium steigert die Viabilität in zwei untersuchten Glioblastom Zelllinien, sogar unter dem Zusatz eines Chemotherapeutikums. Diese Arbeit trägt bei zu unserem bisherigen Verständnis über die Interaktion zwischen mesenchymalen Stammzellen und Glioblastomzellen. Von uns erhobene Resultate unterstreichen den Tropismus der mesenchymalen Stammzellen für die invasiven Areale des Glioblastoms. Gerade diese Strukturen bleiben aufgrund der hohen Migrationsfähigkeit der Tumorzellen nach der neurochirurgischen Resektion im Gehirn zurück. Vor diesem

Hintergrund scheint es besonders interessant, dass mesenchymale Stammzellen die Viabilität der Glioblastomzellen beeinflussen und so maßgeblich am Tumorrückfall beteiligt sind. Mesenchymale Stammzellen und ihre Interaktion mit Glioblastomzellen stellen neue potentielle therapeutische Ansatzpunkte dar, welche zukünftig in der Therapie des Glioblastoms von großem Nutzen sein könnten.

## Abstract

Among other cell lines of the tumor microenvironment, mesenchymal stem cells play an important role in glioma progression. However, many diverging aspects were shown throughout the complex interaction between mesenchymal stem cells and tumor cells. The first part of this work investigated in the migration of injected mesenchymal stem cells in glioblastoma. Furthermore, this study aimed to model one pathologically relevant aspect of the in vivo interaction between mesenchymal stem cells and glioma cells under simplified in vitro conditions in order to analyze a potential effect on the viability of glioma cells.

First, mice were intracranially inoculated with glioma cells. Once the tumor had grown for 58 days, mesenchymal stem cells were injected into the brain into the main tumor mass. After sacrificing the mice, brain sections were analyzed with regards to the mesenchymal stem cells location and blood-brain barrier integrity in glioma. Furthermore, an in vitro proliferation assay was performed studying glioma cells viability under serum-free mesenchymal stem cell conditioned medium.

The in vivo experiment shows migration of mesenchymal stem cells to invasive parts of the tumor. It was demonstrated that in these regions the blood-brain barrier is widely intact. Hence, serum-derived factors larger than the size of 70 kDa do not reach the structures where mesenchymal stem cells reside. Consequently, this serum-free situation was modeled in an in vitro proliferation assay. Serum-free medium, which was conditioned by mesenchymal stem cells, enhances viability in two lines of glioma stem cells even under conditions of chemotherapy.

This paper adds to our understanding of the complex interaction between mesenchymal stem cells and glioma cells. The results of the study provide evidence for mesenchymal stem cells tropism for invasive regions of glioblastoma. These invasive regions remain in the brain after neurosurgery, representing the source of tumor relapse. Taken together, these encouraging results suggest that mesenchymal stem cells are able to support tumor relapse formation by improving viability of glioma cells even under conditions of chemotherapy. This makes mesenchymal stem cells and their interaction with glioblastoma promising potential therapeutic targets to evaluate in glioblastoma therapy in the future.

## List of figures

<b>Figure 1: Major features of GBM subtypes according to Verhaak et al. (7)</b> .....	<b>12</b>
<b>Figure 2: Generation of conditioned medium</b> .....	<b>29</b>
<b>Figure 3: Methodology of proliferation assay</b> .....	<b>30</b>
<b>Figure 4: Timetable of in vivo experiment</b> .....	<b>32</b>
<b>Figure 5: Experimental schedule of in vivo experiment</b> .....	<b>36</b>
<b>Figure 6: Mesenchymal stem cells migrate to invasive areas of the tumor</b> .....	<b>37</b>
<b>Figure 7: Mesenchymal stem cells migrate to tumor satellites</b> .....	<b>40</b>
<b>Figure 8: MSCs do not persist in the tumor core</b> .....	<b>42</b>
<b>Figure 9: Blood-brain barrier in invasive areas of GBM appears largely intact</b> .....	<b>44</b>
<b>Figure 10: Increased viability of Line #7 when incubated with conditioned medium (CM)</b> .....	<b>46</b>
<b>Figure 11: Serum-free MSCs conditioned medium increases viability of Line #7 GSCs</b> .....	<b>47</b>
<b>Figure 12: Serum-free MSCs conditioned medium increases viability of Line #4 GSCs</b> .....	<b>49</b>



# List of abbreviations

BBB *Blood brain barrier*  
bFGF *Basic fibroblast growth factor*  
CAF *Cancer associated fibroblast*  
CCL *CC-chemokine ligand*  
CD *Cluster of differentiation*  
CDK *Cyclin-dependent kinase*  
CDKN2A *Cyclin dependent kinase inhibitor 2A*  
CHI3L1 *Chitinase-3-like protein 1*  
CM *Conditioned medium*  
CMV *Cytomegalovirus*  
CNS *Central nervous system*  
CSF *Cerebrospinal fluid*  
CSF1 *Colony stimulating factor 1*  
CT *Computer tomography*  
CXCL *CXC-chemokine ligand*  
EGF *Epidermal growth factor*  
EGFR *Epidermal growth factor receptor*  
FGF *Fibroblast growth factor*  
GABRA1 *Gamma-aminobutyric acid type A receptor alpha 1*  
GBM *Glioblastoma multiforme*  
GSC *GBM stem-like cell*  
H&E *Hematoxylin & Eosin*  
HSC *Hematopoietic stem cell*  
IDH *Isocitrate dehydrogenase*  
IGF1 *Insulin-like growth factor 1*  
IL *Interleukin*  
LOH *Loss of heterozygosity*  
MDM2 *Mouse double minute 2*  
MGMT *O6-Methylguanine-DNA methyltransferase*  
miRNA *Micro ribonucleic acid*  
MOS *Median overall survival*  
MRI *Magnetic resonance imaging*  
MSC *Mesenchymal stem cell*  
NEFL *Neurofilament light*  
NF1 *Neurofibromin 1*  
NPC *Neural precursor cell*  
OLIG *Oligodendrocyte transcription factor*  
PDGFRA *Platelet-derived growth factor receptor A*

PET *Positron emission tomography*  
PI3K *Phosphoinositide 3-kinase*  
PTEN *Phosphatase and tensin homolog*  
PUFA *Polyunsaturated fatty acids*  
RAS *Rat sarcoma*  
Rb *Retinoblastoma*  
RTK *Receptor tyrosine kinase*  
SD *Standard deviation*  
SNP *Small nucleotide polymorphism*  
SOX-2 *Sex determining region Y (SRY)- box 2*  
SPECT *Single photon emission computed tomography*  
SYT1 *Synaptotagmin-1*  
TA-MSC *Tumor-associated mesenchymal stem cell*  
TERT *Telomerase reverse transcriptase*  
TME *Tumor microenvironment*  
TMZ *Temozolomide*  
TP53 *Tumorsuppressorgene TP53*  
TRAIL *Tumor necrosis factor-related apoptosis inducing ligand*  
VEGF *Vascular endothelial growth factor*  
WHO *World Health Organization*

# 1 Introduction

## 1.1 Glioblastoma multiforme

### 1.1.1 Epidemiology and classification

Glioblastoma multiforme (GBM) is a malignant brain tumor of astrocytic origin (1). With an incidence of 3.22 per 100,000, it represents the most frequent malignant primary tumor of the central nervous system (CNS) (1). Expressed in percentages, 48.3% of all malignant CNS tumors are GBM. After meningioma (37.6%) and tumors of the pituitary (16.8%), glioblastoma (14.6%) represents the third most frequently reported subtype of all CNS neoplasia (1). The median overall survival (MOS) is 13.5 months and cumulative 5-year survival is 5.8%, pointing out the poor prognosis for patients with glioblastoma (2). The incidence is higher in man than in woman, with an incidence rate ratio male:female of 1.58 (1). Interestingly, incidence rates are approximately 2 times higher in caucasians than in people of color (1). The incidence of GBM increases with age, reaching a maximum in 75 to 84-year-olds and median age at diagnosis is 65.0 years (1). GBM belongs to a group of tumors which all arise from glial cells including neural stem and progenitor cells (3, 4). These so-called gliomas consist of astrocytoma (like GBM), oligodendroglioma, ependymoma and mixed gliomas (5). Glioblastoma accounts for the majority of gliomas (57.3%) (1). In addition to the histopathological phenotype the World Health Organization (WHO) classification of CNS tumors from 2016 uses molecular characteristics to define tumor subtypes (5). Besides improvements in diagnostic accuracy and patient management it allows for a more accurate determination of prognosis and treatment response. The new classification differentiates between isocitrate dehydrogenase-wildtype (IDH) and IDH-mutant glioblastoma. 90% of glioblastoma are IDH-wildtype, which usually arise de novo (primary GBM) and are more common in patients that are over 55 years old (5). Representing the other 10%, IDH-mutant glioblastoma correspond closely to secondary glioblastoma, and normally occur in younger patients (5). Considering phenotype and genotype, gliomas are graded from I to IV based on their predicted clinical behavior. WHO grade I describes a benign tumor, whereas grade IV is synonymous with the highly aggressive, incurable GBM (6). A further subdivision of GBM based on the clinically relevant molecular changes, has been suggested by Verhaak et al. They differentiate between classical, mesenchymal and proneural type of glioblastoma. The following table highlights their main characteristics (7).

<b>Classical</b>	<b>Mesenchymal</b>	<b>Proneural</b>
<ul style="list-style-type: none"> <li>- Amplification of chromosome 7 and <i>EGFR</i></li> <li>- Deletion of <i>CDKN2A</i></li> <li>- Loss of chromosome 10</li> <li>- Lack of <i>TP53</i> mutation</li> </ul>	<ul style="list-style-type: none"> <li>- Loss of <i>NF1</i></li> <li>- Deletion of <i>PTEN</i></li> <li>- Expression of mesenchymal markers like e.g. <i>CHI3L1</i> and <i>C-MET</i></li> </ul>	<ul style="list-style-type: none"> <li>- Alterations of <i>PDGFRA</i></li> <li>- Point mutation <i>IDH1</i></li> <li>- Mutation of <i>TP53</i>, <i>SOX-2</i>, <i>OLIG2</i></li> </ul>

**Figure 1: Major features of GBM subtypes according to Verhaak et al. (7)**

### **1.1.2 Etiology**

Even though a lot of genetic and environmental factors have been studied, the etiology of GBM remains largely unknown (8). GBM appears to be largely sporadic (8). However, some risk factors, like genetic alterations, hereditary syndromes and ionizing radiation exposure, have been identified (8). As mentioned above, the risk of GBM increases with age, male gender and white ethnicity (9). Furthermore, immune genes, immune factors and some single nucleotide polymorphisms (SNPs) have been discussed to be associated with GBM (10). Genome-wide association studies could link substitutions of single nucleotides at different loci in the DNA to higher susceptibility to glioma (11). Other risk factors that are connected with GBM are tallness and high socioeconomic status (10). History of asthma or allergy is confirmed to be a protective factor across all histologic grades of glioma (12). Lifestyle features, e.g. smoking cigarettes, drinking alcohol, consumption of drugs and mobile phone use, could not be linked to development of GBM (10).

### **1.1.3 Histopathology**

The majority of glioma are found in the cortical hemispheres. Some are located infratentorial and only few grow in other parts of the CNS than the brain (1, 13). Extraneural metastasis in glioma is very rare (0.2%) (14). Macroscopically, GBM appear heterogeneous with multifocal hemorrhage, necrosis, and cystic and gelatinous areas. Normally they manifest as single, relatively large, irregular shaped lesion that diffusely infiltrates into the surrounding brain parenchyma. The invasive histology of glioblastoma includes a pleomorphic and poorly differentiated cell population with nuclear atypia and mitotic activity (15). In addition, one of

the two following criteria must be fulfilled to confirm the diagnosis of glioblastoma multiforme: microvascular proliferation and/or necrosis (16). Manifestation of necrosis can vary from small multiple regions radially surrounded by glioma cells in a “pseudopalisading” pattern, to large ischemic areas of necrotic vessels and tumor cells (17). The presence of large necrotic regions correlates with a poor clinical outcome (17). Another major characteristic feature of GBM is proliferation of vascular endothelial cells with glomeruloid structures (18). It is not possible to distinguish between a primary or secondary tumor by analyzing the glioblastoma’s morphology. While the histology remains largely homogenous, GBM consist of distinct subtypes exhibiting significant heterogenic features on a molecular level. This explains why a diagnosis based solely on histopathology is insufficient (16). Nevertheless, three special subtypes, namely giant cell glioblastoma, epitheloid glioblastoma and gliosarcoma can be defined (5).

#### **1.1.4 Pathogenesis**

In order to improve the poor outcome in patients suffering from glioma, researchers started to shed light on the tumor pathogenesis in recent years (19). They began to focus on molecular aberrations to better understand the development of GBM. To provide a short and simplified overview, the main aspects of tumorigenesis of GBM are pointed out.

In general, three major pathways have been identified by the Cancer Genome Atlas to be altered in GBM: receptor tyrosine kinase (RTK)/rat sarcoma (RAS)/Phosphoinositide 3-kinase PI3K, Retinoblastoma (Rb) and p53 signaling pathway (20). Integrative analysis show that these pathways are mutated in 88%, 87% and 79% of GBM, respectively (20).

The most frequent alterations of the RTK/RAS/PI3K pathway can be detected in epidermal growth factor (EGFR) and in the phosphate and tensin homolog (*PTEN*) gene (20). Overexpression of EGFR, especially the specific mutation EGFRvIII, leads to increased cell proliferation and survival. PTEN blocks the pathways triggered by EGFR, thereby inhibiting cell proliferation. If PTEN is mutated, tumorigenesis is enhanced (4).

The Rb protein controls the cell cycle by preventing its progression from G1 to S-phase (4). This tumor suppressor protein can be phosphorylated and thereby inactivated by cyclin-dependent kinase (CDK) 4 and 6. These enzymes are normally inhibited by the proteins of the *CDKN2A* gene. In conclusion, mutations of the *CDKN2A* gene lead to a stronger tumor growth (21).

The P53 pathway plays a key part in secondary glioblastoma, as it is detectable in most of low-grade diffuse astrocytoma (22). As a tumor suppressor protein, the p53 protein plays an

essential role in several “cellular processes, including the cell cycle, response of cells to DNA damage, cell death, cell differentiation, and neovascularization” (23). Hence, mutations of this gene enhance tumor development. Overexpression of mouse double minute 2 (MDM2) results in inactivation of p53 and is associated with primary GBM (4).

As already mentioned, GBM can be subdivided in primary and secondary glioblastoma. The most frequent genetic alteration (60-80%) in both types of GBM is loss of heterozygosity (LOH) 10q, the long arm of chromosome 10 (24). Without 10q the cell has lost various genes that encode for tumor suppressor proteins playing significant roles in pathogenesis of glioblastoma (4).

Primary GBM arises de novo without any signs for clinical and histological precursor lesions (4). They are of the IDH1/2 wildtype and grow rapidly and invasively in older patients. Characteristic hallmark modifications for primary GBM include EGFR gene amplification, deletion of p16, telomerase reverse transcriptase (TERT) promoter mutation, overexpression of MDM2 and PTEN aberrations (15). *PTEN* gene is located on chromosome 10q and is therefore affected by LOH (15).

On the other hand, secondary glioblastoma develops less rapidly after malignant transition from low-grade or anaplastic astrocytoma (4). Secondary GBM is of the IDH1/2 mutant genotype and correlates with alterations of TP53 and ATRX, LOH of 19q and overexpression of platelet derived growth factor A and alpha (PDGFA; PDGFa) and retinoblastoma (Rb) (15).

Another aspect that is worth mentioning is the clinically relevant O6-Methylguanine-DNA methyltransferase (MGMT) methylation. MGMT is a protein that is able to repair DNA, therefore protecting cells against tumorigenesis induced by alkylating agents (4). Moreover, this protein is also capable of protecting mutated tumor cells against alkylating chemotherapeutics, such as Temozolomide (TMZ) (25). If the MGMT promoter region is methylated, thereby inhibiting transcription of MGMT, the glioblastoma cells are more sensitive to TMZ (4). In conclusion, “patients with glioblastoma containing a methylated MGMT promoter were shown to have a substantially greater benefit from adjuvant temozolomide treatment” (25).

### **1.1.5 Diagnosis**

The mean duration from showing first symptoms to a concrete diagnosis is 6.3 months, whereas secondary glioblastoma develop over several years (26). The average time of progression from low grade glioma or anaplastic glioma to GBM is around 2 years and 5 years, respectively. Mean age of diagnosis is 62 years (primary GBM) and 45 years (secondary GBM) (26). As generally symptoms progress quite rapidly, it is important to rule out other acute neurological diseases like intracranial bleeding for instance.

The symptoms are varied and often non-specific. They range from focal neural deficits (40-60%) to headaches (30-50%) and seizures (20-40%) (15). Within and around the lesion, brain tissue becomes dysfunctional due to necrosis. Depending on the tumor localization, symptoms can be diverse. If the tumor is located in the temporal lobe, it can affect the auditory and visual system, whereas the occurrence of personality changes indicate that a lesion is located in the frontal lobe. Severe cases also present gait imbalance, urinary retention and hemiparesis (27). Over time, tumor growth and peritumoral edema result in increased intracranial pressure. As a consequence, patients might suffer from headaches, nausea and vomiting. It is therefore essential to pay close attention to the history of headaches. Red flags that may indicate the presence of a brain tumor are progressive severity, unilateral localization and new onset in over 50-year-olds (27). Occasionally, seizures can be the first clinical symptom and usually a focal onset is reported (28).

If there is a suspicion of glioblastoma, neuroimaging has to be performed as a diagnostic measure. Normally, patients undergo brain magnetic resonance imaging (MRI) with and without contrast media in order, to visualize anatomic features of the lesion (29, 30). A computed tomography (CT) scan is performed in patients with contraindications for MRI, e.g. pacemakers (27). The tumor appears hypointense in T1-weighted MR images and hyperintense in T2-weighted scans (30). After injection of gadolinium, the irregularly shaped, inhomogeneous lesion typically shows a central region of necrosis, surrounded by perifocal edema (31). The lesions usually occur unifocal but can be multifocal. Brain metastases or brain abscess are possible differential diagnosis (27). In recent years other nuclear medicine techniques, such as positron emission tomography (PET) or single photon emission computed tomography (SPECT), have helped to draw a more precise picture of the tumor (15).

### 1.1.6 Therapy

To date, the treatment of glioblastoma remains challenging, and even though extensive research is being carried out on new therapy options, GBM is still a devastating diagnosis with a poor outcome. Standard therapy includes maximal surgical resection, radiotherapy and chemotherapy (18).

Since GBM grow highly invasive, the tumor cannot be resected completely. As a result, tumor cells remain in the brain which consequently leads to tumor relapse. Nevertheless, patients with glioblastoma undergo radical surgery (32). This lowers the intracranial pressure and neurological deficits can disappear. Moreover, cytoreduction reduces seizure incidence and provides tissue for histologic and molecular tumor characterization. This ultimately improves life quality and additional therapy of the patients (32).

In order to target remaining cancer cells, adjuvant radiotherapy is started within 4 to 6 weeks after surgical treatment. The standard radiotherapy dose is 60 Gy divided in 30 daily fractions over 6 to 7 weeks (32). The ionizing radiation causes DNA double strand breaks followed up by necrosis of the damaged cells (33).

The third important pillar of treatment is chemotherapy. In 2005 Stupp et al. could show that concomitant use of Temozolomide (TMZ) improves median overall survival when compared to radiation alone. Median survival of patients taking TMZ is 14.6 months, whereas without TMZ the MOS is 12.1 months (34). As mentioned, therapy with TMZ is more effective in patients with MGMT-methylated tumors (25). Latest research results have suggested an additional use of lomustine in patients with methylated MGMT promoter region (35). TMZ is an alkylating agent, that is taken orally every day during radiation and 5 times a month afterwards for the following 6 months. Its function lies in methylating purine and pyrimidine in DNA, resulting in apoptosis. As TMZ can cause thrombocytopenia and lymphopenia, it is important to check on blood parameters and possibly modify dose and schedule (36). In some cases, the immunosuppressive effect of TMZ leads to infection with *Pneumocystis jirovecii*, a fungus causing life-threatening pneumonia (37). The once promising monoclonal antibody, Bevacizumab, could not show an improvement of survival in larger randomized trials (38). Bevacizumab, binding to vascular endothelial growth factor (VEGF), is only considered as an option in patients with nonresectable tumors (39).



Beside tumor treatment it is important to reduce patients symptoms caused either by treatment or the tumor itself. Depending on the clinical context, corticosteroids like dexamethasone can be used in order to decrease intracranial pressure (40). As corticosteroids show immunosuppressive effects, it must be evaluated whether the patients risk of infectious diseases is appropriate (40). Levetiracetam is an efficient and commonly used antiepileptic drug in patients who experience seizures due to glioma (41). To prevent patients from nausea and vomiting caused by chemotherapy, a 5-HT<sub>3</sub> receptor antagonist like ondansetron has been proven to be useful (42).

## **1.2 Mesenchymal stem cells**

Recent studies have underlined the influence of nonmalignant, stromal cells in the tumor microenvironment (43). Tumors form organ-like tissues, comprising not only tumor cells, but also non-cancerous, genetically stable stromal cells (43). This includes fibroblasts, immune cells, endothelial cells and many more (44). Likewise, mesenchymal stem cells (MSCs), a heterogeneous group of stromal progenitor cells, can be identified as part of this complex tumor tissue (45, 46).

Reporting the identification of colony forming fibroblast units, Friedenstein et al. were the first to describe MSCs in 1970 (47). Since then, a considerable amount of literature demonstrated that MSCs reside in almost all tissues of the body, such as e.g. bone marrow or adipose tissue (48). As the definition of stem cells indicates, MSCs possess the ability of self-renewal and multipotent differentiation into various cells of the mesodermal lineage, such as osteocytes, chondrocytes and adipocytes. MSCs, also defined as mesenchymal stromal cells, are able to transdifferentiate, meaning that they have the capacity to transform into cells from unrelated germline lineages (48-50).

In order to identify mesenchymal stem cells, a panel of cell biological properties and surface markers are taken into account. Firstly, they are capable of differentiating into osteocytes, adipocytes and chondrocytes in vitro (51). Secondly, they grow adherently in plastic flasks under standard culture (51). The third criterium is the expression of surface proteins CD73, CD105, and CD90 and absence of CD45, CD43, CD79alpha or CD19, CD14 or CD11b, and HLA-DR receptor (51). However, several studies reveal that the tissue of origin modifies MSCs properties in terms of differentiation potential, proliferative rate, and marker expression profile (52, 53). Moreover, MSCs from different organs comprise different lineage commitment

depending on their original *in vivo* environment. For example, ectopic transplantation of bone marrow derived MSCs leads to formation of ectopic bone tissue, whereas dental pulp-derived MSCs form odontogenic tissue (53, 54). In the bone marrow, MSCs represent an essential element of the hematopoietic stem cell (HSC) niche. They support HSC homeostasis and control differentiation and proliferation of the HSCs. Hence, they regulate HSCs quiescence and release of mature progeny (55). In addition, perivascular MSCs could be found to reside in neurovascular niches of the human brain along with neurons, endothelial cells and astrocytes (56, 57). MSCs closely resemble pericytes and a perivascular origin for MSCs is hypothesized (58).

Furthermore, MSCs play a key role in tissue regeneration. Caplan and Correa have extensively studied MSCs migration, specifically to wounds (59). They demonstrate their integration into injured tissues and their subsequent participation in local repair mechanisms. MSCs are able to modulate the inflammatory response of the damaged microenvironment and initiate proliferation of tissue stem cells through the secretion of chemokines, growth and immunoregulatory factors (59, 60). Conclusively they suggest “that MSCs may serve as site regulated “drugstores” *in vivo*” (59). As a matter of fact, MSCs have been successfully applied in the treatment of chronic inflammatory diseases or chronic wounds (61). A study by Zhang et al. claims that human umbilical cord MSCs improve liver function and ascites in patients suffering from severe liver cirrhosis (62). Another trial involving 16 patients with systemic lupus erythematosus reveals promising effects of human umbilical MSCs by a significant reduction of disease activity in all patients (63).

In addition, it was found that MSCs migrate to tumor sites and convert into tumor associated MSCs (TA-MSCs) and cancer associated fibroblasts (CAFs) (64). Interestingly, several *in vivo* studies have reported MSCs homing for glioma (65, 66). In order to study migration of MSCs *in vivo*, innovative tracking methods like bioluminescent optical imaging or magnetic resonance imaging have been used (67). They all describe MSCs tropism for glioma (68, 69). Indeed, in their recent review Liu et al. suggest that MSCs are capable of crossing the blood brain barrier (BBB) (70).

At this moment, 501 MSC-based studies are listed according to the clinical trial registry of the US National Institute of Health (Search terms: mesenchymal stem cells OR mesenchymal stromal cells; recruiting, not yet recruiting, active not recruiting on 6<sup>th</sup> of December 2021) (71).

This shows that much work on the potential of MSCs is being carried out, yet little is known about the interaction between MSCs and glioma. Comprehension of the complex ways in which GBM cells interact with their surroundings, not only within the tumor but with the whole organism, is pivotal for an effective cancer prevention and therapy (72).

### **1.3 Aim of thesis**

In the last decade the tumor microenvironment of glioblastoma has become more and more relevant. Endogenous non-mutated cells and genuine tumor cells are interacting constantly in several complex ways (43). This has an impact on tumor expansion, invasiveness and resistance to therapy. Previous studies identified mesenchymal stem cells as part of the tumor microenvironment in GBM (45). Further research projects regarding the interaction with glioblastoma have shown a pathological role of tumor associated MSCs (73). In vitro cell culture results describe a tumor supportive effect of MSCs under serum-free conditions (74). It is critical to shed light on the conditions MSCs are confronted with. For this reason, it is important to investigate the locations MSCs migrate towards in order to identify the conditions under which MSCs reside in vivo. Additionally, the interaction of MSCs conditioned medium and glioma cells is examined regarding viability and chemoresistance. The aim of this thesis contains an analysis of the following questions:

1. Can locoregional differences in MSC migration be identified in a preclinical tumor model of GBM?
2. If MSC migration is locoregionally different in a tumor model, can histopathological characteristics in these different tumor regions be defined?
3. Do MSCs affect glioma growth?
4. If so, can reasons or certain factors be identified that are involved in the supposed effects of MSCs on GBM?

## 2 Material and Methods

### 2.1 Material

#### 2.1.1 Devices & Softwares

<b>Material</b>	<b>Supplier</b>
Countess II FL <i>Cell Counting Machine</i>	Thermo Fisher Scientific
Centrifuge	Heraeus
Table Top Centrifuge	Eppendorf
Incubator	Binder
Magnetic Hot Plate Stirrer	VWR International
Microtome	PFM Medical
Perfusion System	Integra Biosciences
Pipettor Accujet Pro	Brandt
Isopropanol-submerged Cryovial Holder	Sigma-Nalgene
Shaker	Biozyme Scientific
Stereotactic Operation Device	
Vortex Mixer	VWR
Zeiss Axioskop 2 Light Microscope	Carl Zeiss Microscopy
Zeiss Axiovert 25 Fluorescence Microscope	Carl Zeiss Microscopy

Leica Confocal Laser Microscope SP8 Upright Confocal 405/WLL Phys Stand Malpighi	Leica Microsystems
Graph Pad Prism 6.0	Graph Pad software, Inc.
LAS X Core offline version	Leica Microsystems
Image J	NIH
Adobe Photoshop	Adobe Inc.

### 2.1.2 In vitro: Cell culture

Material	Supplier	Cat #
Dulbecco's Modified Eagle Medium (DMEM)	Biochrom	FG0415
DMEM F12	ThermoFischer Scientific	11320033
Neurocult Basal Medium (NBM)	Stemcell Technologies	05700
Neurocult Proliferation Supplement	Stemcell Technologies	05701
B27	ThermoFischer Scientific	17504044
Minimal Essential Medium Non-essential Aminoacids (MEM NEAA)	ThermoFischer Scientific	11140068
Penicillin/Streptomycin	ThermoFischer Scientific	15140122
hEGF (10ng/ml)	ThermoFischer Scientific	PHG6045
FGF (10 ng/ml)	ThermoFischer Scientific	PHG0263
Accutase	Stemcell Technologies	07920

Trypsin	Biochrom GmbH	L 2123
Phosphate-buffered Saline (PBS) sterile	Apotheke Klinikum der Universität München	-
Trypan Blue Solution (0,4%)	Sigma Aldrich	T 8154
Countess cell counting chamber slides	invitrogen by Thermo Fisher Scientific	C10283
Counting Chamber Neubauer	Paul Marienfeld GmbH&Co.KG	0640110
Aqua	Braun Melsungen AG	67240920000
Dimethylsulfoxide (DMSO)	Emsure ACS Merck KGaA	317275
Temozolomide	Sigma Life Science	T2577
Tissue Culture Flask T25	TPP	90026
Tissue Culture Flask T50	TPP	90076
Tissue Culture Flask T150	TPP	90151
6 Well Plates	TPP	92406
Bacillol AF Surface Disinfectant	Hartmann	973380
Stripette 5ml	Corning Incorporated	4487
Stripette 10ml	Corning Incorporated	4488
Stripette 25ml	Cellstar greiner bio-one	760180
Cryotubes	Kischer Biotech	CV11-2

15 ml Falcon	TPP	91015
50 ml Falcon	TPP	91051
Tubes 0.5 ml 1 ml 2 ml	Eppendorf	20030121.023 0030121.694 0030120.094
Wypall	Kimberly Clark	2061349

### 2.1.3 In vivo: Animal experiment

Material	Supplier	Cat #
Scalpel	Feather	FB10
Microliter syringe	Hamilton	1710SL
Syringe 1 ml	Braun	9166017V
Nylon 5 – 0 Suture	Ethicon	1855G
Bepanthen Augen und Nasensalbe <i>Eye cream</i>	Bepanthen	82290583
Ethanol 70%; 96%; 100%	Apotheke Klinikum der Universität München	-
PBS, sterile	Apotheke Klinikum der Universität München	-
Syringe Needle 30G	BD Microlance	3054000
Ketamidor <i>100 mg/ml Ketamin</i>	WDT	4025270000
Rompun 2% <i>Xylazine</i>	Bayer	62938410000

NaCl 0.9%	Fresenius Kabi Deutschland	69488220000
Dextran, biotin, 70 kDa	Thermo Fisher Scientific	2161929
Paraformaldehyde (PFA)	Sigma Aldrich	P6148-500G

## 2.1.4 Histology

### 2.1.4.1 Tissue preparation

Material	Supplier	Cat #
Sucrose	Sigma Aldrich	S0389
Shandon Cryomatrix Frozen Embedding Medium	Thermo Fisher Scientific	6769006
Tissue Tek Cryomold	Sakura	4566
Glycerol	Sigma Aldrich	G5516
Ethylene glycol	Sigma Aldrich	324558
Parafilm "M"	Bemis	PM-999

### 2.1.4.2 H&E (Hematoxylin and Eosin) Staining

Material	Supplier
100% Ethanol	Apotheke Klinikum der Universität München
Hemalaun	Carl Roth
Eosin G Solution	Sigma Aldrich



Roti-Histol	Carl Roth
Entellan Mounting Medium	Merck

#### 2.1.4.3 Immunohistochemistry

<b>Material</b>	<b>Supplier</b>	<b>Cat #</b>
TWEEN 20	GERBU Biotechnik	2001.0250
Triton-X	Fluka	93418
4',6-Diamidino-2-phenylindole DAPI	Fluka	32670
Normal Donkey Serum	Jackson Immuno Research	017-000-121
Alexa Fluor 647 conj. Streptavidin	Jackson Immuno Research	016-600-084
Alexa Fluor 488 Donkey anti-goat	Jackson Immuno Research	705-545-147
Microscope Slides Superfrost Ultra Plus	Thermo Scientific	J 3800 AMNZ
Cover glass, 24x50 mm	LLG Labware	9.160829
Fluorescence Mounting Medium	Dako	S3023

## 2.2 Methods

### 2.2.1 In vitro: Cell Culture

#### 2.2.1.1 Cell lines

##### Cells

Line #4  
**classical**

Line #7  
**proneural**

GBM stem like cells (GSCs) were isolated from human glioblastoma biopsies, cultured under stem cell conditions and genetically characterized regarding stem cell properties. Afterwards, their gene expression profile was analysed and the tumor cells were classified in subtypes. Line #4 belongs to the classical subtype, whereas Line #7 represents a proneural subtype. These two cell lines were obtained by Galli et al. from a collaborating laboratory in Italy. For further information see their article published in Cancer Research in 2004 (75).

m0007\_A  
**mesenchymal**

NPCs (Neural Precursor cells) were derived from the subventricular zone of mice (p53 KO, NF1 fl/fl, PTEN fl/fl). Isolated cells were cultured under stem cell conditions and further transduced with pcLV-CAG-PDGFB-IRES-CRE-NLS-CMV-CopGFP-T2a-Puro vector from Sirion Biotech company and afterwards selected with Puromycin. Subsequently, the Cre enzyme cuts off NF1 and PTEN sequences (loxP sequences), the GFP sequence encodes for a green fluorescent protein and the cells express PDGFB. They were proven to be tumorigenic upon orthotopic implantation in mice.

mMSC-  
CMV DsRed

Murine bone marrow derived MSCs from C57BL/6 mice were purchased from Thermofischer Scientific. Subsequently they were transduced with a CMV DsRed vector. This vector contains a reporter gene that encodes for a red fluorescent protein under the control of the cytomegalovirus (CMV) (74).

### 2.2.1.2 Medium composition

<b>Cells</b>	<b>Medium</b>
Line #4	Neurocult Basal Medium 445ml, Neurocult Proliferation Supplement
Line #7	50ml (10%), Penicillin/Streptomycin 5ml (1%), 10 ng/mL EGF (Epidermal Growth Factor), 10 ng/mL FGF (Fibroblast Growth Factor)
m0007_A	DMEM/F12 485ml, B27 10ml (2%), Penicillin/Streptomycin 5ml (1%), 10 ng/mL EGF, 10 ng/mL FGF
mMSC-CMV DsRed	DMEM 390ml, FCS 100ml (20%), Penicillin/Streptomycin 5ml (1%), MEM NEAA 5ml (1%)

### 2.2.1.3 Glioma stem cell culture

GBM stem like cells (GSCs) were maintained either in NeuroCult Basal Medium or DMEM/F12 (for detailed information of medium composition see above, section 2.2.1.2). The cells were kept at 37°C in an incubator with humidified atmosphere of 5% CO<sub>2</sub>. As GSC cultures grow, they build spheroids. Splitting was necessary every second to fourth day depending on the growth rate of the different cell lines. In the first step GSC suspension was transferred into 15 ml tubes and centrifuged at 400 x g for 5 minutes. The supernatant medium was removed and the cells were resuspended in 1 ml of accutase solution. Accutase is an enzyme with proteolytic and collagenolytic activity, therefore acting as a cell detachment inducing agent (76). After adding accutase, the cells were dissociated by gently pipetting. Then, the suspension was put in a water bath at 37°C for 3-5 minutes and finally dissociated by pipetting. Afterwards, GSCs were washed with 2 ml of proper cell culture medium and centrifuged for an additional 5 minutes at 400 x g. The supernatant liquid was removed and the cells were gently dissolved in fresh medium at an appropriate density specific for each cell line. All the GSCs were cultured in normal cell culture flasks.

### 2.2.1.4 Mesenchymal stem cell culture

Mesenchymal stem cells are adherent, fibroblast-like shaped cells (77). They were maintained in DMEM (supplied with 20% FBS) and kept at 37°C in an incubator with humidified atmosphere of 5% CO<sub>2</sub>. At a confluent stage of 80-90% the cells were trypsinized in order to prevent them from overgrowing and culture dying. First, the medium was discarded and then

the cells were washed with PBS to remove cell detritus and remaining FCS. Once Trypsin was added to the cells (1ml for T25; 3ml for T75; 5ml for T150), the flask was swung gently back and forth to cover the monolayer. Afterwards, the flask was incubated for at least 3 minutes at 37°C. The enzyme Trypsin breaks down adhesion-proteins between either cells or between cells and the culture flask. If cells did not detach properly, the flask was carefully tapped to bring them into suspension. In order to inactivate Trypsin, DMEM (double amount of Trypsin) was added and the cell suspension was put in a 15 ml tube and centrifuged at 400 x g for 5 minutes. Finally, the supernatant was removed and the MSCs were resuspended in the appropriate amount of fresh Medium (5ml for T25; 10ml for T75; 20ml for T150). Passaging is carried out every 3 days.

#### 2.2.1.5 Freezing cells

It is important to keep stocks of low passage cells, because these cells resemble the original cell line more closely (78). Hence, cells at low passages were frozen in aliquots at -80°C until they were used. For this purpose, a particular freezing medium including 10% DMSO in DMEM/F12 (for MSCs: DMEM) without additives was prepared. Once the cells built big spheroids in the T150 flasks they were ready to be frozen up. This was not necessary with adherent MSCs. Cells were transferred to a 15 ml tube, centrifuged and the supernatant medium was removed. The cells were dissolved in their respective medium (without additives). 500 µl of this cell suspension and 500 µl of the freezing medium were mixed. In the final mixture the DMSO concentration was 5%. Finally, the cells were stored in Isopropanol-submerged cryovial holders at -80°C. The holders reduce the risk of ice crystal formation, which may damage the cells and eventually cause cell death.

#### 2.2.1.6 Cell counting

Throughout my experiments, cells were counted both manually and with a cell counter. Cells were centrifuged, split and finally dissolved in 1ml of the respective culture medium. Then 20 µl of the cell suspension were taken out and homogeneously mixed with 20 µl of Trypan Blue to dye cells (1:2 solution). From this solution 10 µl was transferred to a counting grid (Neubauer for manual counting, Countess Chamber slides for cell counting machine). In order to count the cells manually a microscope was used; to count them automatically the grid was inserted in the counting machine. The results are given as the total amount of cells in 1ml medium.

### 2.2.1.7 Conditioned medium (CM)

Conditioned medium was kindly provided by Spitzweg group from Medizinische Klinik und Poliklinik IV of LMU Klinikum. MSCs (L87/4; Passage 21) were cultivated in DMEM without FCS (as mentioned above, murine MSCs were normally kept in a medium containing FCS) for 72 hours and then the medium was harvested. Conditioned medium was then stored at -20°C until used. The L87/4 cell line was established by Thalmeier et al at the LMU Klinikum in 1994 by immortalizing bone marrow MSCs via SV40 large T antigen (79).

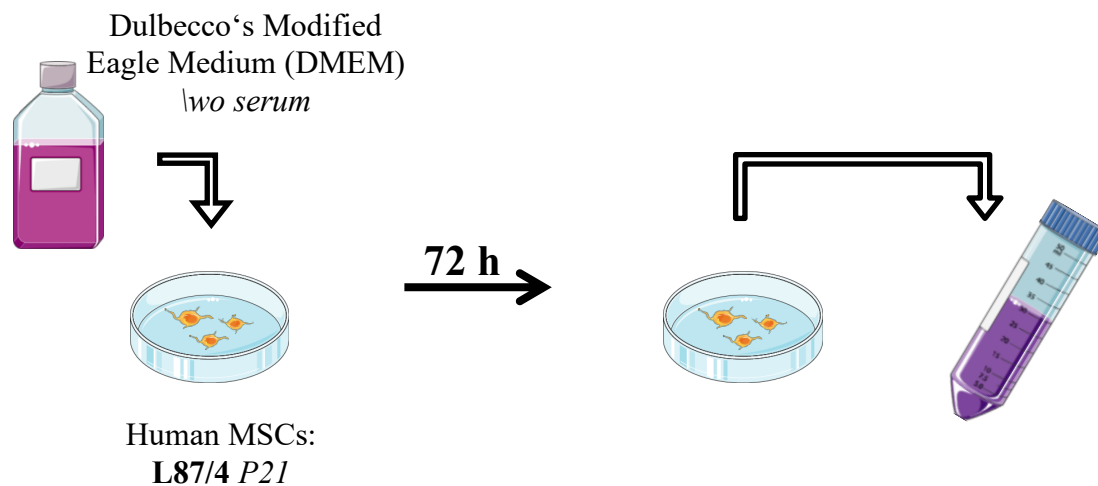


**Figure 2: Generation of conditioned medium**

### 2.2.1.8 Proliferation assay/Cell counting assay

Initially, Temozolomide (TMZ; 25mg) was dissolved in 429  $\mu$ l of DMSO and then mixed with 5359  $\mu$ l of DMEM. In order to completely dissolve the TMZ powder, vortexing was required for at least 20 minutes. In the end the TMZ concentration was 25mM.

In a 6-well-plate, 100,000 cells per well were plated. The cells were either dissolved in MSC-CM or DMEM and subsequently TMZ (100  $\mu$ M: 8  $\mu$ l; 300  $\mu$ M: 24  $\mu$ l) was added in every well except for the TMZ-free groups. In total, 6 conditions (CM: 0; 100; 300  $\mu$ M TMZ, DMEM: 0; 100; 300  $\mu$ M TMZ), with 3 replicates each were prepared. These plates were incubated at 37°C, 5% CO<sub>2</sub>/95% humidified air. The medium was changed twice after 24 hours and after 48 hours, dissolving the cells again in the same condition that they were in before. After 72 hours the cells were put back into their regular culture medium Neurocult Basal Medium (NBM) with supplements. The cells were counted on day 7 and 100,000 cells were plated back in their regular culturing medium (NBM) with supplements into each well. After 14 days the cells were counted the second time and once again 100,000 cells were put back into each well. On day 21

the third and last counting was performed. The cell number on day 14 and 21 was calculated by extrapolating from the sample of 100,000 cells to the total amount. The results are presented as the mean  $\pm$  SD of 3 independent experiments.

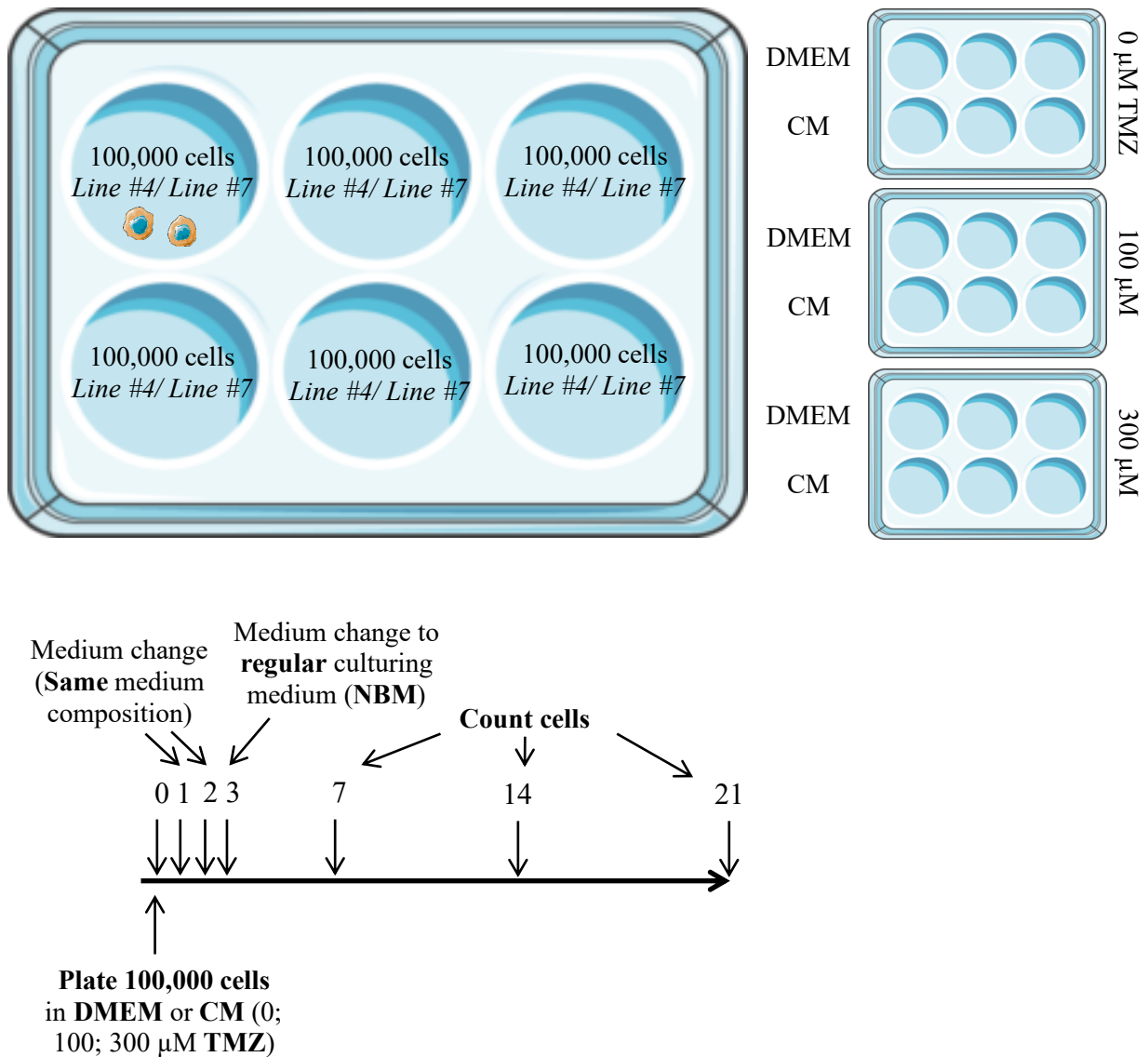


**Figure 3: Methodology of proliferation assay**

In each well 100,000 glioma cells (Line #4/Line #7) were plated in either MSC Conditioned Medium (CM) or Dulbecco's Modified Eagle Medium (DMEM) as a control without TMZ, with 100  $\mu$ M and 300  $\mu$ M of TMZ, respectively. The timetable of the experiment is indicated below. On day 1 and 2 the medium was changed and the cells were dissolved in the same medium condition that they were in before. On day 3 the cells were put back into their regular culturing medium Neurocult Basal Medium (NBM) with supplements. On day 7, 14 and 21 cells were counted.

## **2.2.2 In vivo: Animal experiment**

### **2.2.2.1 Animals**

The animal experiment was approved by the local animal care committee of the Government of Oberbayern and conducted following animal welfare regulations (including 3R principle) of the National Guidelines for Animal Protection in the Walter-Brendel-Centre of Experimental Medicine at the Ludwig-Maximilians-Universität München. The laboratory mice (strain: CR C57/B6) lived in standardized cages in a 12 h light/dark cycle with access to enough food and water. They were inspected every day after surgery.

### **2.2.2.2 Anesthesia**

In order to perform inoculation and perfusion, mice were anaesthetized. Initially, 1.02 ml of Ketamidol (Ketamine), 0.36 ml of Rompun 2% (Xylazine) and 4.86 ml of NaCl 0.9% was mixed together in a 15 ml tube. For the inoculation of cells 7 µl/g of this anesthetic mix was injected intraperitoneally. In order to apply a lethal injection, 14 µl/g was administered. Several minutes after injection adequate anesthesia was ensured by pinching a paw. If no reflexes could be observed the mouse was ready to undergo surgery. During all surgical interventions eye cream was carefully put on the eyes of the mice to prevent them from drying out.

### **2.2.2.3 Inoculation**

Murine GBM cells (m0007\_A) and murine MSCs (mMSC CMV DsRed) were inoculated intracranially in 3 anesthetized immunocompetent mice at two different points of time, yet the inoculation procedure was the same. On day 0 50,000 cells of m0007\_A were injected into the mice brains (2 mm right/1 mm anterior from bregma). Past experiments of our research group have shown that MSC do not survive the time necessary for the tumor to grow even though the reasons behind this are unclear. Therefore MSCs (100,000 cells) were inoculated into the tumor mass one week prior to killing and perfusing the mice (2 mm right/0.5 mm posterior from bregma).

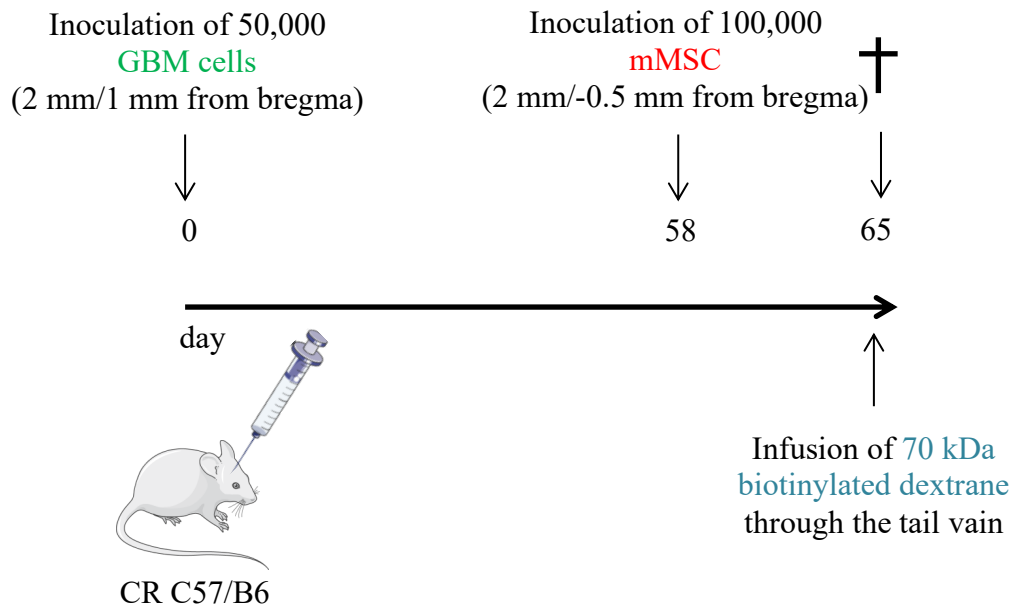


**Figure 4: Timetable of in vivo experiment**

Before inoculation it was required to set up the stereotactic device and to ensure that the block on which the mice were laying was in the correct position in order to minimize neck torsion and prevent occlusion of blood vessels. Then all surgical equipment was sterilized by placing them into a heater for about 10 minutes. Afterwards the surgical equipment was disinfected. The sterilization of Hamilton syringe went as follows. First rinse in 98% ethanol, next in 70% ethanol, next in 50% ethanol, next in sterile water and finally in sterile PBS.

When the mouse was completely anesthetized, the scalp was disinfected with Iodine. After that the scalp was cut longitudinally and centrally between the ears, about 1-2 cm in order to reveal the bregma. Next, the mice were placed into a stereotactic device and the head was secured. Coming from the bregma, the spot where cells were intended to be injected was identified. In my experiment this was 2 mm laterally right and 1 mm in rostral direction for the m\_0007A inoculation. For the mMSC injection the spot was 2 mm laterally to the right and 0.5 mm in occipital direction from the bregma. There, a hole was drilled into the skull using a drill or a large gauge needle. Now the Hamilton syringe was inserted 4 mm deep into the brain through the hole and half of the cells were injected. After waiting for one minute the second half of the cells was injected. After waiting for another one minute the syringe is retracted one mm at a time, waiting for one minute after each mm retracted. Finally, the scalp was sutured and the mice were put back into the cage. It was checked whether the cage contains enough food and water.



#### 2.2.2.4 Dextrane Infusion and Perfusion

Before sacrificing mice on day 65, biotinylated dextrane was injected intravenously in order to study vessel leakage in the mice brains (80). Once the mice were anaesthetized with 7 µl/g of the above described anesthetic mix, 70 kDa large biotinylated dextrane was administered through the tail vein. Afterwards mice were narcotized with a lethal dose of the anesthetic mix. Then, mice were fixed on a styrofoam board. Their chest was cut open carefully and paraformaldehyde (PFA) 4% was injected by a pump into the left ventricle of the heart and a little hole was cut in the right atrium. The still beating heart supported by the pump distributed the PFA in the body and brain. After 15 ml of transcardially infusion of PFA 4% the skull was opened, and the brain was removed.

### 2.2.3 **Histology**

#### 2.2.3.1 Tissue preparation

After successful removal, the brains were maintained in a 4% PFA solution for 48 hours at 4°C to fix the tissue. Then, the brains were soaked VE water, containing 30% sucrose, for 48 hours or until they sank to the bottom of the tube. The brains were frozen in liquid nitrogen and transferred to a mold filled with cryomatrix embedding medium and kept for at least one day at -20°C. Now the frozen brains were ready to be cut. Using a microtome, the parenchyma was cut in 40 µm thick horizontal sections. In a 24 well plate, in which the wells were filled with a cryoprotection solution, the brain sections were preserved while freely floating. Subsequently, the plates were covered with Parafilm “M”. The cryoprotection solution contained two parts PBS, one part glycerol and one part ethylene glycol. This prevents the brain sections from freezing as the well plates were stored at -20°C until further use.

#### 2.2.3.2 H&E (Hematoxylin & Eosin) Staining

The H&E staining is one of the principal tissue stains in histology, which colors acid structures blue and acidophile (basic) structures pink. The staining was conducted as follows to give an overview of the brain section and its tumor.

First of all, the free-floating sections were mounted on a cover slide. Once the slides have dried, they were dehydrated in 100% Ethanol for 30 seconds. The slides were transferred to Hemalaun for 1 minute before they were rinsed in running tap water for 5 minutes. The sections were counter stained with 0.5% Eosin solution for 1 minute. After shortly dipping the slides in VE water, they were dehydrated with 70% Ethanol for 20 seconds. After that, the slides were

dehydrated with 96% Ethanol and 100% Ethanol for one minute each before they were put in Roti-Histol for one minute. Finally, the slides were covered with Entellan and a cover slide.

#### 2.2.3.3 Immunohistochemistry

Selected brain slice sections were washed three times for 5 minutes in PBS Tween (0.1% Tween 20). The primary antibody was diluted in a protein blocking solution in an antibody dependant concentration. The concentration of primary antibody to protein blocking solution was 1:200. The protein blocking solution was composed of 0.3% Triton with 5% donkey serum. The primary antibody mixture was transferred to as many wells as desired in a 24 well plate (500  $\mu$ l/well). Normally, each well was stocked with 4-5 brain slice sections. The sections were incubated overnight at 4°C in the primary antibody solution.

The next day, brain sections were washed again as mentioned before in PBS Tween. The sections then were transferred to the secondary antibody dilution. Again, the antibody was diluted in the protein blocking solution in the correct antibody diluting factor. The ratio between secondary antibody and protein blocking solution was 1:500. The secondary antibody binds to the primary antibody and carries a fluorescent protein that is detected later under the microscope. The brain sections were incubated in the secondary antibody solution for 2 hours on the shaker protected from light. After that the sections were washed once again in PBS Tween as mentioned above. The staining of biotinylated 70 kDa dextrane only required one antibody, because the “primary” antibody, biotin, is already attached to dextrane. Streptavidin, a biotin binding protein, acted as the secondary antibody. It is covalently bound to the fluorescent marker Alexa Fluor 647.

In a PBS bath the sections were put on microscope slides with the help of a brush. After letting the slides dry for around 15 minutes, 4',6-diamidino-2-phenylindole (DAPI) was put on the brain until every part was covered. DAPI was diluted in PBS in a concentration 1:50.000. After 5 minutes the slides were dipped in VE Water. Finally, the slides were mounted: 2-3 drops of mounting medium was added on top of the slides and a coverslip was used to seal the slides.

#### 2.2.4 **Microscopy**

HE stained brain slice sections were analyzed under a Zeiss Axioskop 2 light microscope. Immunostained sections were evaluated with a fluorescence and a confocal microscope. All confocal images were acquired with the Leica confocal laser microscope SP8 Upright Confocal 405/WLL Phys Stand. With a 40X objective lens a merged overview comprised of several

images was conducted. Sequentially Z stacks of representing parts of these overviews were acquired (Zoom in factor was set to 2-3). The format of every image taken was 1024 x 1024 pixels. Confocal images were processed with the help of LAS X Montage Imaging software and Image J.

In order to study microscopy images according to a pattern, a rough categorization in “tumor center” and “invasive tumor areas” was taken into account. First, a complete H&E-stained mouse brain section was analysed to identify the main tumor mass. This tumor bulk appears like a basophile structure with a high cell density. A confocal image of this region shows numerous irregular shaped nuclei and a typical strong green fluorescent signal. In the following this part is called the tumor center.

On the other hand, in peripheral regions of the tumor, where the transition to healthy brain tissue is fluent, less nuclei can be found and the cell density decreases. In order to examine if tumor cells exist in these invasive parts, a confocal image is required. If green fluorescent tumor cells can be clearly identified, these regions are called invasive areas of the tumor.

### **2.2.5 Statistical analysis**

All statistical analyses were conducted using GraphPad Prism 6.0. Each variable was summarized in its distribution by using the mean (SD). The number of repetitions of independent experiments is described in the text of each figure (n). In order to assess the statistical differences between groups one-way ANOVA was performed. P values are as well described in the text of each figure (P value). A Bonferroni post-hoc test of preselected columns was used for the determination of statistical significance. Values were again reported as the mean  $\pm$ SD.

Statistical significance was defined as  $p < 0.05$  for a 95% confidence interval. P values are indicated as \*,  $p < 0.05$ ; \*\*,  $p < 0.005$ ; \*\*\*,  $p < 0.0005$  in all results.

### 3 Results

#### 3.1 Mesenchymal stem cells migrate to invasive areas of the tumor

In Figure 6 the H&E-stained image of a complete horizontal mouse brain slice section clearly shows the tumor bulk in the right hemisphere. It appears as a basophile structure with a high cell density.

The H&E-stained image in Figure 7 displays another complete horizontal mouse brain slice section, which is cut more caudally than the H&E-stained image in Figure 6. A small basophile structure, a tumor satellite, can be found in the left hemisphere occipital of the ventricle.

Figure 6 and Figure 7 demonstrate that mMSCs migrate to invasive tumor regions or tumor satellites. In fact, tumor satellites also represent invasive parts of the tumor. Hence, one can state that mMSCs migrate to invasive areas of the tumor. Before inoculation, mMSCs were transduced with a CMV DsRed vector. This vector contains a reporter gene that encodes for a red fluorescent protein under the control of the cytomegalovirus (CMV) (74). In both Figures, Figure 6 and Figure 7, B and C show magnifications of mMSCs and additionally provide an orthogonal view (z-level). Here, mMSCs are identified in close apposition to GBM cells (Figure 6C; Figure 7B, C).

In conclusion, mMSCs can be observed in the pathophysiological microenvironment of invasive tumor areas. Subsequently, it is important to shed light on this exact tumor microenvironment as it might influence mMSCs behavior.

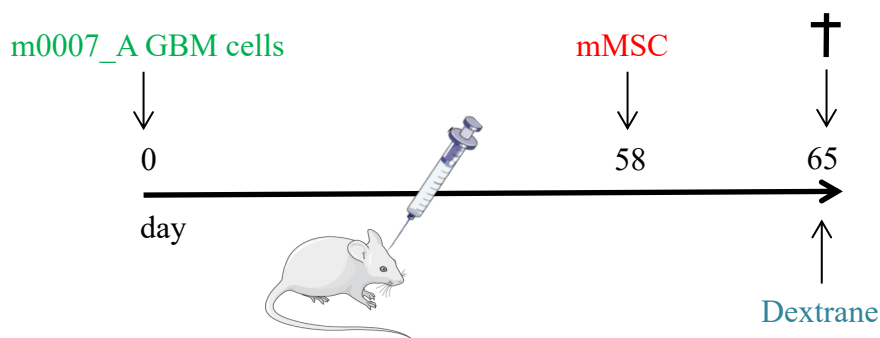


**Figure 5: Experimental schedule of in vivo experiment**

For further information see methods part.

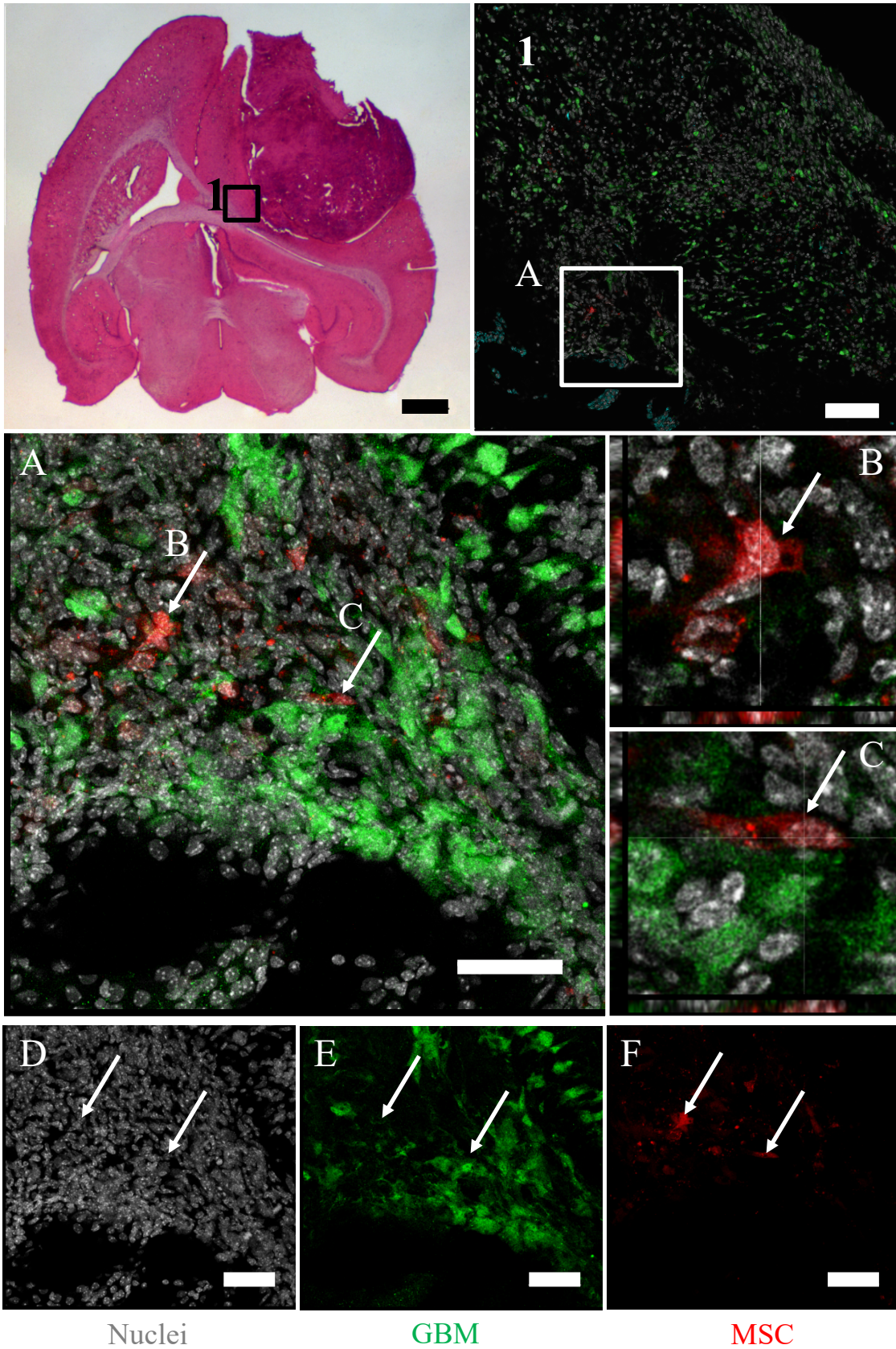
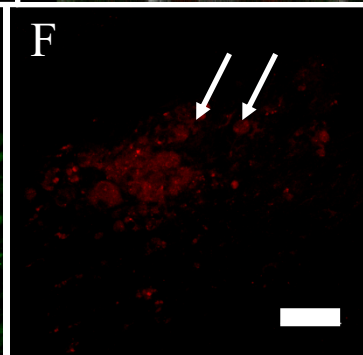
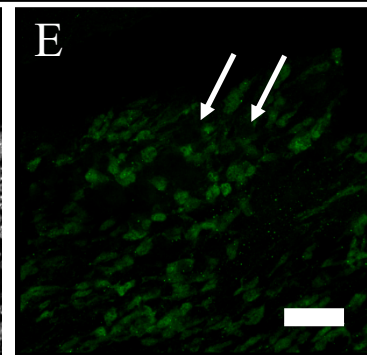
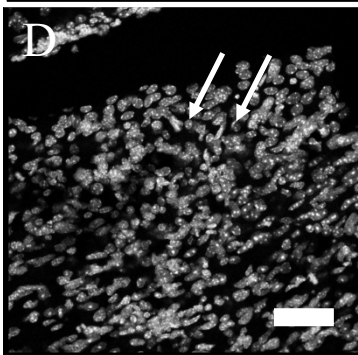
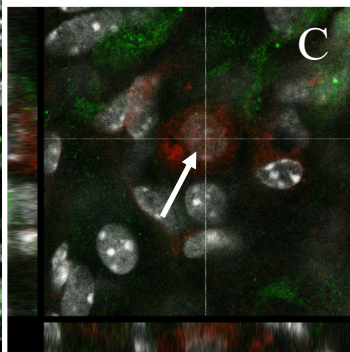
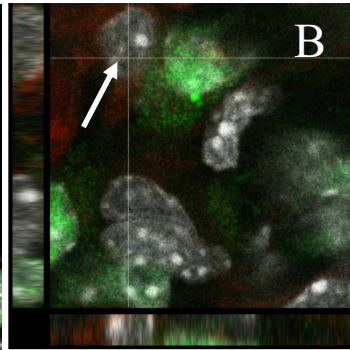
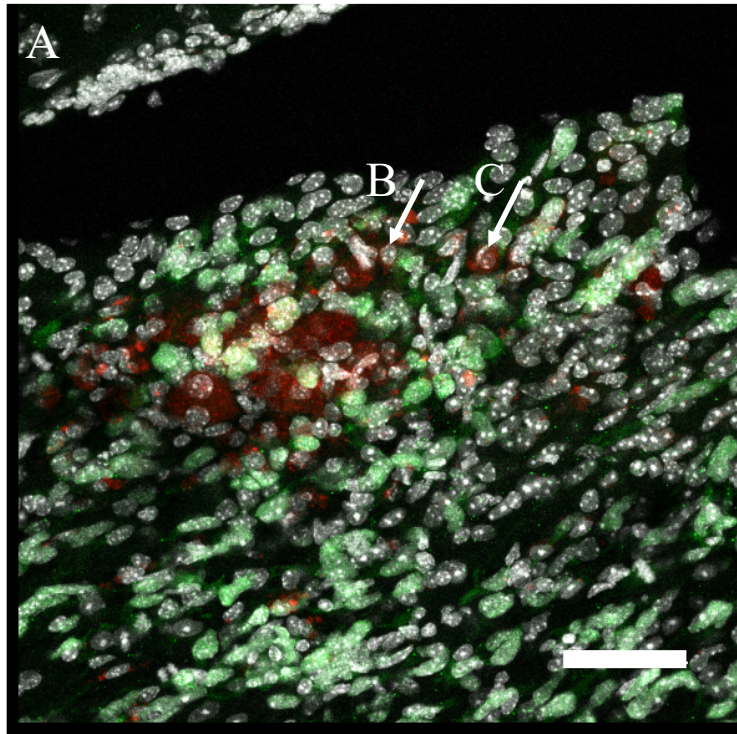
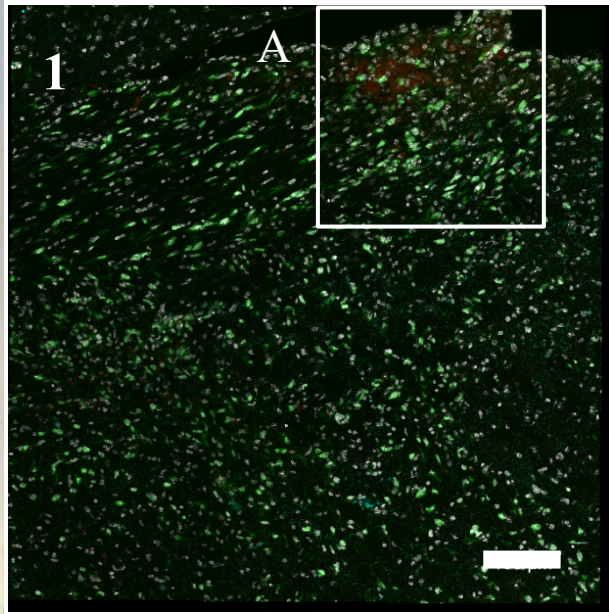


**Figure 6: Mesenchymal stem cells migrate to invasive areas of the tumor**

The first image shows a complete H&E-stained mouse brain slice section in an axial plane (Scale bar: 1000  $\mu\text{m}$ ). The marked square (1) represents an invasive area of the tumor and refers to the confocal image on the right (1; Scale bar: 100  $\mu\text{m}$ ). The region of interest is then highlighted (A) and shown in the picture below (A; merged channels; Scale bar: 20  $\mu\text{m}$ ). Two mMSCs are marked with an arrow. These two mMSCs are magnified in B and C. Magnification C shows that mMSCs are found in close apposition to GBM cells. Images D (Nuclei), E (GBM) and F (MSC) represent the separate channels of merged image A

(Scale bar: 20  $\mu\text{m}$ ). Before inoculation, both cell lines, m\_0007A GBM cell line and mMSC line, were transduced with a vector containing a reporter gene that either encodes for a green (m\_0007A) or a red (mMSC) fluorescent protein. As the Figure indicates, numerous mMSCs migrate to invasive areas of the tumor.



Nuclei

GBM

MSC

**Figure 7: Mesenchymal stem cells migrate to tumor satellites**

The images are in identical order as in Figure 6. They show the same findings in another part of the mouse brain and more important of the tumor. In the H&E-image (Scale bar: 1000  $\mu\text{m}$ ) an invasive tumor satellite is marked with a black square (1). This region is represented with a confocal image on the right (1; Scale bar: 100  $\mu\text{m}$ ). The region of interest is highlighted (A) with a white triangle and shown in the picture below (A; merged channels; Scale bar: 20  $\mu\text{m}$ ) Again, two mMSCs are marked with an arrow. These two mMSCs are magnified in B and C. Both magnifications show that mMSCs are in close apposition to GBM cells. Images D (Nuclei), E (GBM) and F (MSC) represent the separate channels of merged image A (Scale bar: 20  $\mu\text{m}$ ). Before inoculation, both cell lines, m\_0007A GBM cell line and mMSC line, were transduced with a vector containing a reporter gene that either encodes for a green (m\_0007A) or a red (mMSC) fluorescent protein. This Figure shows that mMSCs migrate to invasive tumor satellites.



### **3.2 MSCs do not persist in the tumor core**

In contrast, no mMSCs could be identified in the tumor center at this timepoint in my experimental schedule. mMSCs were injected intracranially on day 58 after tumor inoculation and mice were sacrificed on day 65. Remarkably, mMSCs were only found in invasive tumor parts. In the MSC channel in Figure 8C no red signal can be detected, demonstrating that inoculated mMSCs don't reside in the tumor center at this timepoint.

Nevertheless, with my experimental schedule it is not possible to make a statement about the migration of endogenous MSCs as they obviously do not express RFP.

Figure 8A and Figure 8B show the typical distribution pattern of nuclei and tumor cells in the tumor center. Both nuclei and cells are very numerous and irregularly shaped, some are small, others are long and narrow.

All in all, my experiments could show that the interaction of MSCs and GBM cells is stable at invasive zones of glioma, whereas the MSC half-life seems to be short in the tumor center.

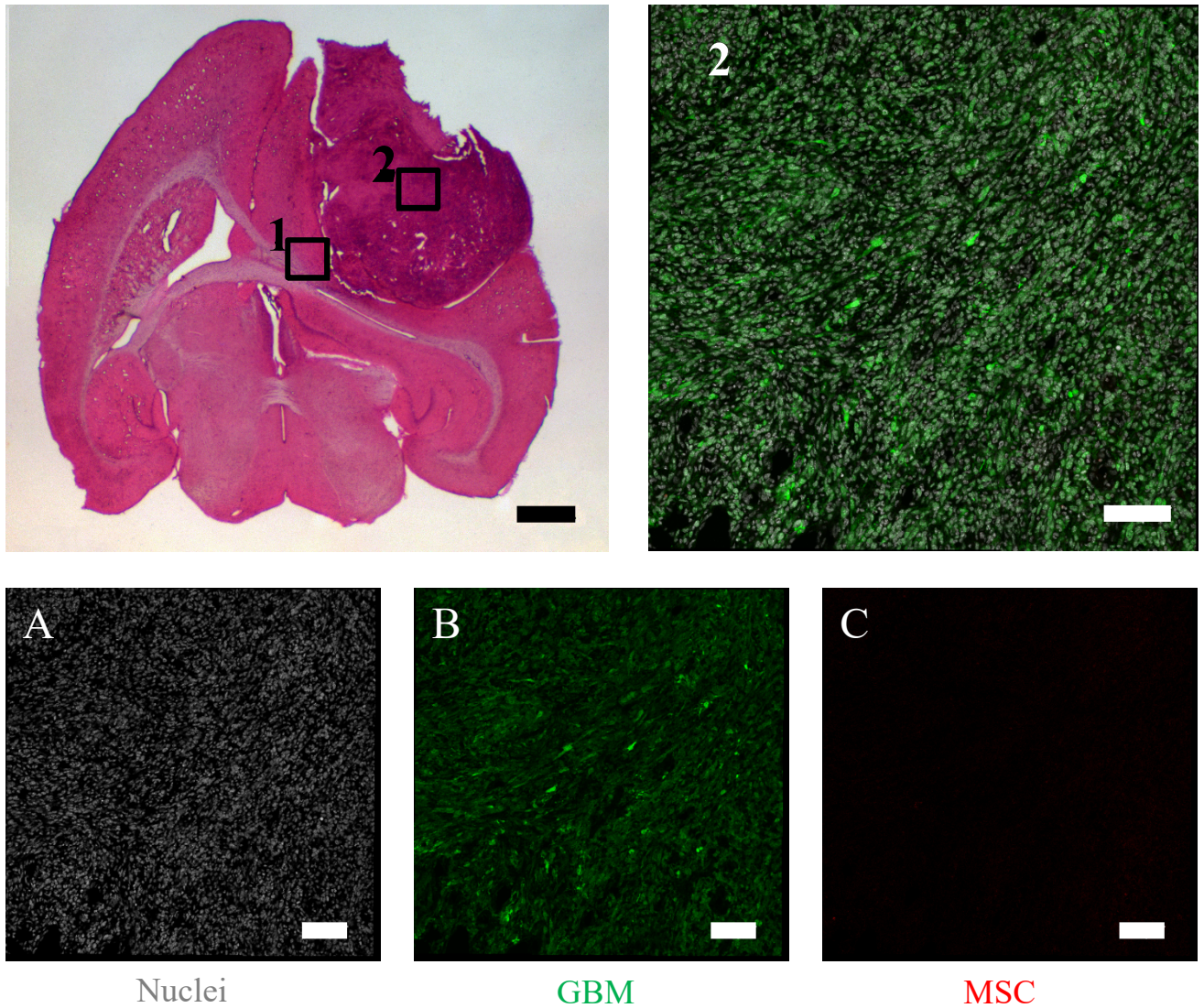


**Figure 8: MSCs do not persist in the tumor core**

The H&E-stained image above is the same brain slice section as already shown in Figure 6 (Scale bar: 1000  $\mu\text{m}$ ). Rectangle 1 marks the invasive area of the tumor. Rectangle 2, on the other hand, marks the tumor center and refers to the merged confocal image on the right (2; Scale bar: 100  $\mu\text{m}$ ). Images A (Nuclei), B (GBM) and C (MSC) show the separate channels (Scale bar: 100  $\mu\text{m}$ ). Before inoculation, both cell lines, m\_0007A GBM cell line and mMSC line, were transduced with a vector containing a reporter gene that either encodes for a green (m\_0007A) or a red (mMSC) fluorescent protein. No red signal can be detected in C, demonstrating that inoculated mMSCs don't reside in the tumor center at this timepoint in my experimental schedule. A and B show the typical distribution pattern of nuclei and tumor cells in the tumor center. Both nuclei and cells are very numerous and irregularly shaped, some are small, others are long and narrow.

### **3.3 Blood-brain barrier in GBM invasive areas appears largely intact**

Figure 9 shows the leakiness in invasive tumor areas compared to the leakiness in the tumor center. In invasive tumor areas no clear dextrane signal can be detected (Figure 9 A3, Figure 9 B3). The weak signal only represents background fluorescence. In contrast, in the tumor center a strong intensive dextrane signal can be found (Figure C3). Here, dextrane enters the GBM microenvironment due to a defective blood-brain barrier (BBB) (81). If the BBB is dysfunctional due to tumor expansion, tissue destruction or cell necrosis, dextrane (70 kDa large) is able to cross the BBB to enter the GBM microenvironment (81). For this reason, dextrane is a tracer for leakiness of the BBB and a strong dextrane signal stands for elevated leakiness and extravasation. This can be observed in the main tumor mass, whereas in invasive tumor areas the BBB seems to be widely intact.

Not only the dextrane channel shows a stronger signal in the tumor center. In addition, a higher cell density and cell number in Figure 9 C2 than in Figure 9 A2 and and Figure 9 B2 is found. Moreover, the green-fluorescent signal in the tumor center (9 C1) is strong, speaking for a highly tumor cell infiltrated area. A close look to the bottom of Figure 9 A3 reveals a small dextrane uptake. This signal displays the choroid plexus. As it produces and secretes the cerebrospinal fluid (CSF), the composition of the barrier between blood and CSF is different to the BBB under physiological conditions (82). It is called the blood-cerebrospinal fluid barrier and in this case serves as a positive control.

To sum up, the blood-brain barrier seems to be largely intact in invasive areas of GBM. Interestingly, these are the regions where mMSCs reside in my experimental schedule. A dysfunctional BBB allows circulating molecules and pathogens to invade the brain parenchyma and interfere with its cells. The remaining integrity of the BBB in invasive zones of GBM prevents most of the blood-derived serum factors from entering the brain microenvironment.

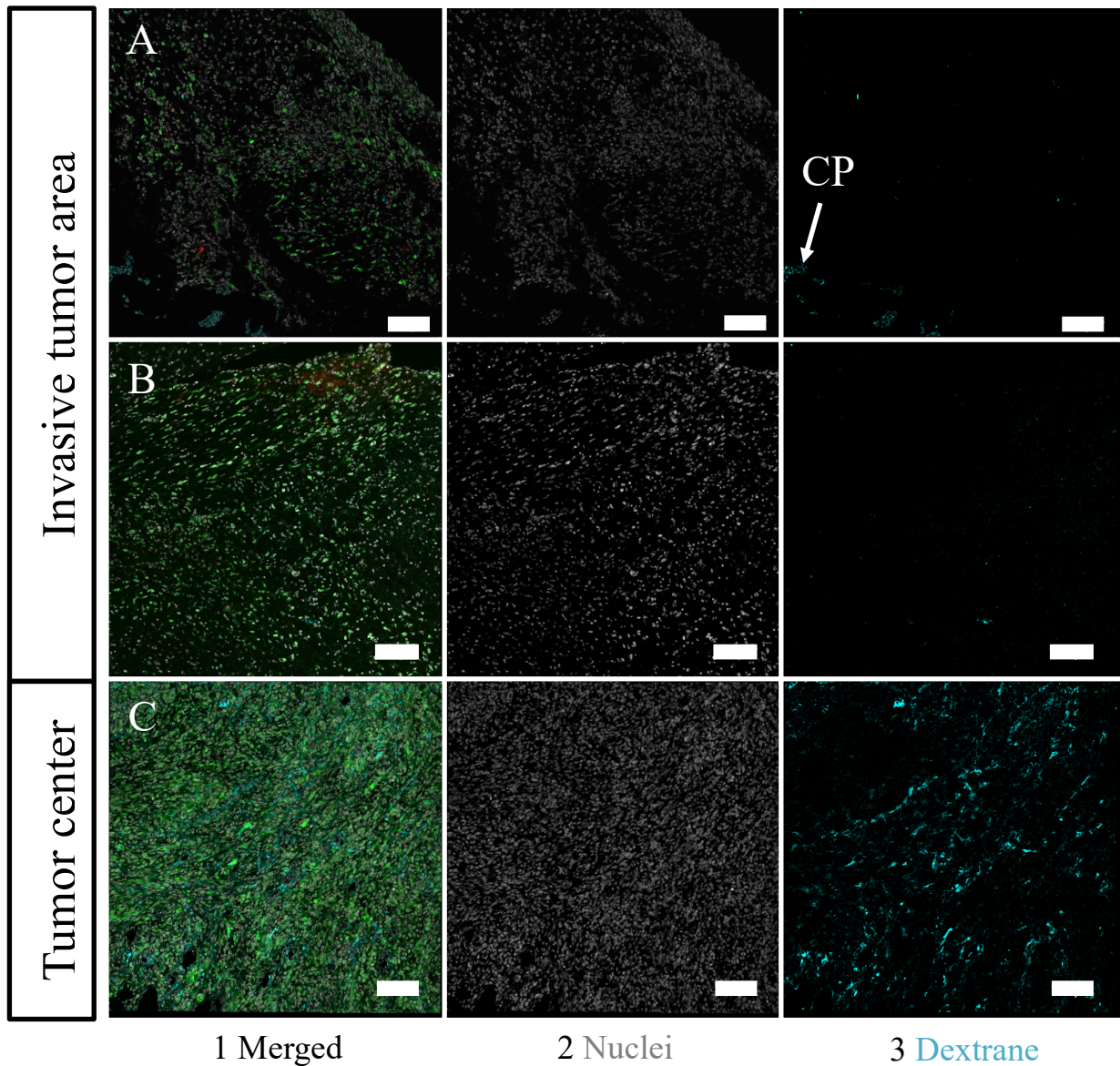


**Figure 9: Blood-brain barrier in invasive areas of GBM appears largely intact**

Horizontally, row A and B represent the invasive tumor area, whereas row C stands for the tumor center. Vertically, the first row (1) are the merged channel images, the second row (2) shows the nuclei channel and the third row (3) represents the dextrane channel. Before sacrificing mice, biotinylated dextrane was injected intravenously in order to study vessel leakage in the mice brains. If the BBB is dysfunctional due to tumor expansion, tissue destruction or cell necrosis, dextrane (70 kDa large) is able to cross the BBB to enter the GBM microenvironment (80). For this reason, dextrane is a tracer for leakiness of the BBB and a strong dextrane signal stands for elevated leakiness and extravasation. 70 kDa biotinylated dextrane is not detectable in A3 and B3. In contrast, a strong dextrane signal can be observed in C3. This speaks for an elevated leakiness and extravasation in the tumor center and no leakiness in invasive tumor areas. This means that the blood-brain barrier in invasive areas in GBM is largely intact. The remaining integrity of the BBB in invasive zones of GBM prevents most of the serum factors from entering the brain microenvironment. In addition, a higher cell density and cell number in C2 than in A2 and B2 is found. Moreover, the green-fluorescent signal in the tumor center (C1) is strong, speaking for a highly tumor cell infiltrated area. Before inoculation, m\_0007A GBM cell line was transduced with a vector containing a reporter gene that encodes for a green fluorescent protein. A close look to the bottom of A3, marked with a white arrow reveals a small dextrane uptake. This signal displays the choroid plexus (CP) and in this case serves as a positive control. The scale bar in every image is 100  $\mu\text{m}$ .

### **3.4 Serum-free MSCs conditioned medium increases viability of GSCs**

In the tumor center mMSCs may eventually accumulate but appear to have a short half live, as no mMSCs could be detected in the tumor center in my in vivo experimental schedule. Anyway, mMSCs may be pathologically important in the main tumor mass, but this mass is surgically resected. However, invasive tumor areas remain after surgery and due to a functional blood-brain barrier may represent brain areas not exposed to serum factors. That is why for the following in vitro studies, the serum-free situation was modeled.

In my in vitro experiment viability of GSCs was analyzed with a proliferation assay by counting cells after certain time points. In order to generate CM, human MSCs were cultivated in DMEM medium without serum factors for 72h. The serum-free condition is supposed to affect the MSCs secretome, and thereby the CM.

Afterwards, two different cell lines of GSCs (Line #7 and Line #4) were incubated with either conditioned medium or a control medium in order to observe possible pro- or antiproliferative effects mediated by secreted factors of MSCs. GSCs were exposed to CM or the control medium for 72 hours and then transferred to their regular culturing medium. GSCs were counted on day 7, 14 and 21 (Figure 10A).

In addition, a chemotherapeutic drug that is commonly used against GBM, temozolomide (TMZ), was added in different concentrations to the groups in order to study chemoresistance of GSCs. The conditioned medium might contain factors that induce chemoresistance in GSCs. This gets even more important, considering the situation after surgical resection of the main tumor mass. TMZ is a chemotherapeutic drug used in GBM therapy and usually given after surgical treatment in order to kill remaining glioma cells. It is crucial to find out if MSCs induce insensitivity in glioma cells to TMZ as it might strongly influence a successful therapy.

First of all, the graph lines in Figure 10B highlight that, for cell Line #7 after 7, 14 and 21 days in every group with conditioned medium the cell number is higher than in the groups cultured with DMEM. The graph line for the means of CM 300  $\mu$ M TMZ is even higher than the means of DMEM without TMZ. The cell number in groups with CM increases faster, especially in the first 7 days. After 7 days the cell number of groups CM and DMEM rise approximately in an equal manner. In sum, the graph indicates a transient effect of the CM. This transient impact appears to be delayed for the CM 300  $\mu$ M TMZ group.

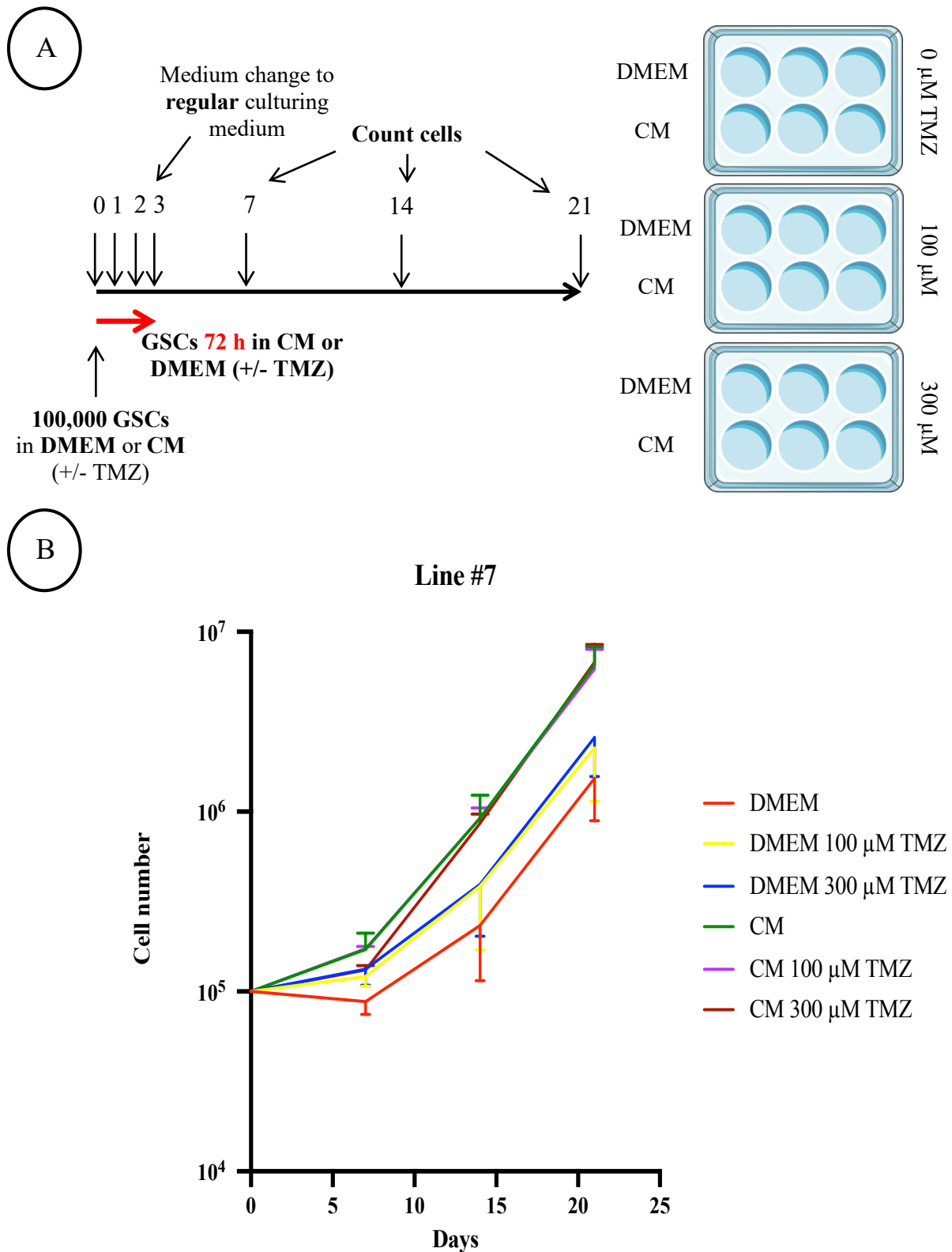


**Figure 10: Increased viability of Line #7 when incubated with conditioned medium (CM)**

Experimental details are explained in A. GSCs Line #7 was exposed to either MSCs conditioned medium (CM) or a control medium (DMEM) for 72h. Additionally, TMZ was applied in different concentrations in order to study chemoresistance. After 72h, GSCs were transferred back to their regular culturing medium and cells were counted on day 7, 14 and 21. B shows the measured viability for Line #7. Time is indicated as days on the X axis. Every line graph in B represents a condition of the mentioned ones on the right. The Y axis represents the cell number in log scale. The graph lines represent the means and the standard deviation is indicated as a small bar (only in one direction for a better clarity). (n=3) After 7, 14 and 21 days in every group with conditioned medium the cell number is higher than in the groups cultured with DMEM.

The following bar charts portray the difference in cell numbers on day 14 and 21 for Line #7. For each diagram, one-way ANOVA was performed in order to analyze the variance of all groups. Afterwards, Bonferroni post-hoc test was carried out in order to compare preselected columns.

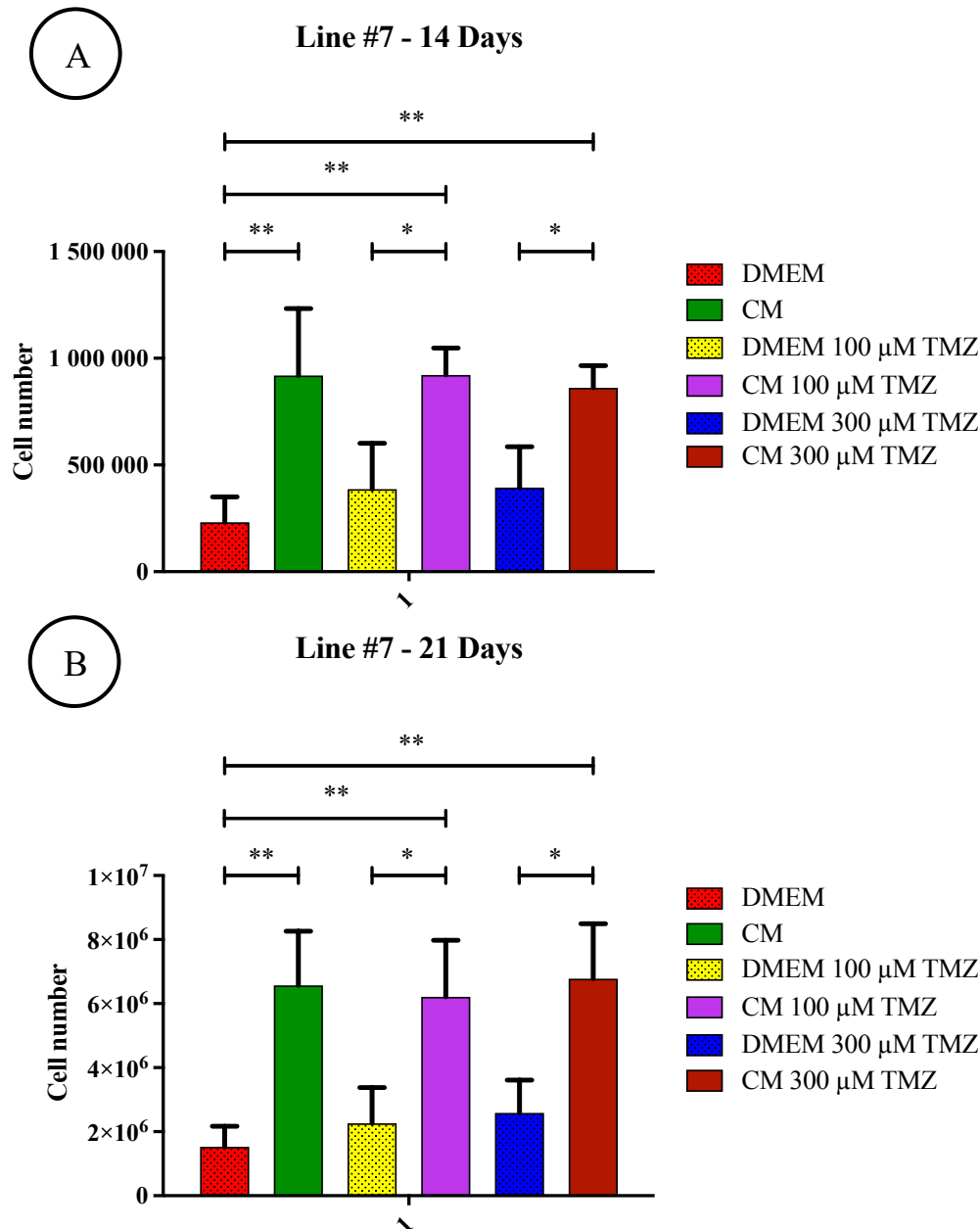


**Figure 11: Serum-free MSCs conditioned medium increases viability of Line #7 GSCs**

The bar charts show the viability measured in cell number of Line #7 on day 14 (A) and on day 21 (B). Every column represents a condition of the mentioned ones on the right. Results are illustrated as the mean  $\pm$  SD. On both days, day 14 and 21, the cell number of the groups CM without TMZ is higher than the corresponding control group. Even under conditions of chemotherapy the difference between CM groups with 100 and 300  $\mu$ M and their corresponding DMEM groups with TMZ is considerable on both days. The Y axis represents the cell number in log scale. One-way ANOVA between all groups was performed first (A: P value: 0.0016 (\*\*); B: P value 0.0009 (\*\*\*)). Afterwards, Bonferroni test was carried out in order to compare preselected columns. Statistical significances are indicated in the figure: \*,  $p < 0.05$ ; \*\*,  $p < 0.005$ ; \*\*\*,  $p < 0.0005$ . (n=3)

On both days, day 14 and 21, the cell number of the groups CM without TMZ is more than three times as large as the corresponding control group. As indicated in Figure 11A and 11B, this difference is significant on both days (\*\*). The difference in viability between CM groups with 100 and 300  $\mu$ M TMZ and their corresponding groups DMEM with 100 and 300  $\mu$ M TMZ is considerable on both days (Figure 11A \*, \*; Figure 11B \*, \*). It is to note that group CM 100  $\mu$ M TMZ and group CM 300  $\mu$ M TMZ represent a significant higher cell number each than group DMEM without TMZ on both days (Figure 11A \*\*, \*\*; Figure 11B \*\*, \*\*).

All in all, conditioned medium increases viability of GSC Line #7. Nevertheless, Line #7 is largely insensitive to TMZ and CM augments cell numbers irrespective of the presence of TMZ. There is no evidence for chemoresistance induced by CM.

The following bar charts portray the difference in cell numbers on day 14 and 21 for Line #4. Again, one-way ANOVA was performed for each diagram in order to analyze the variance of all groups and Bonferroni post-hoc test was carried out afterwards in order to compare preselected columns.



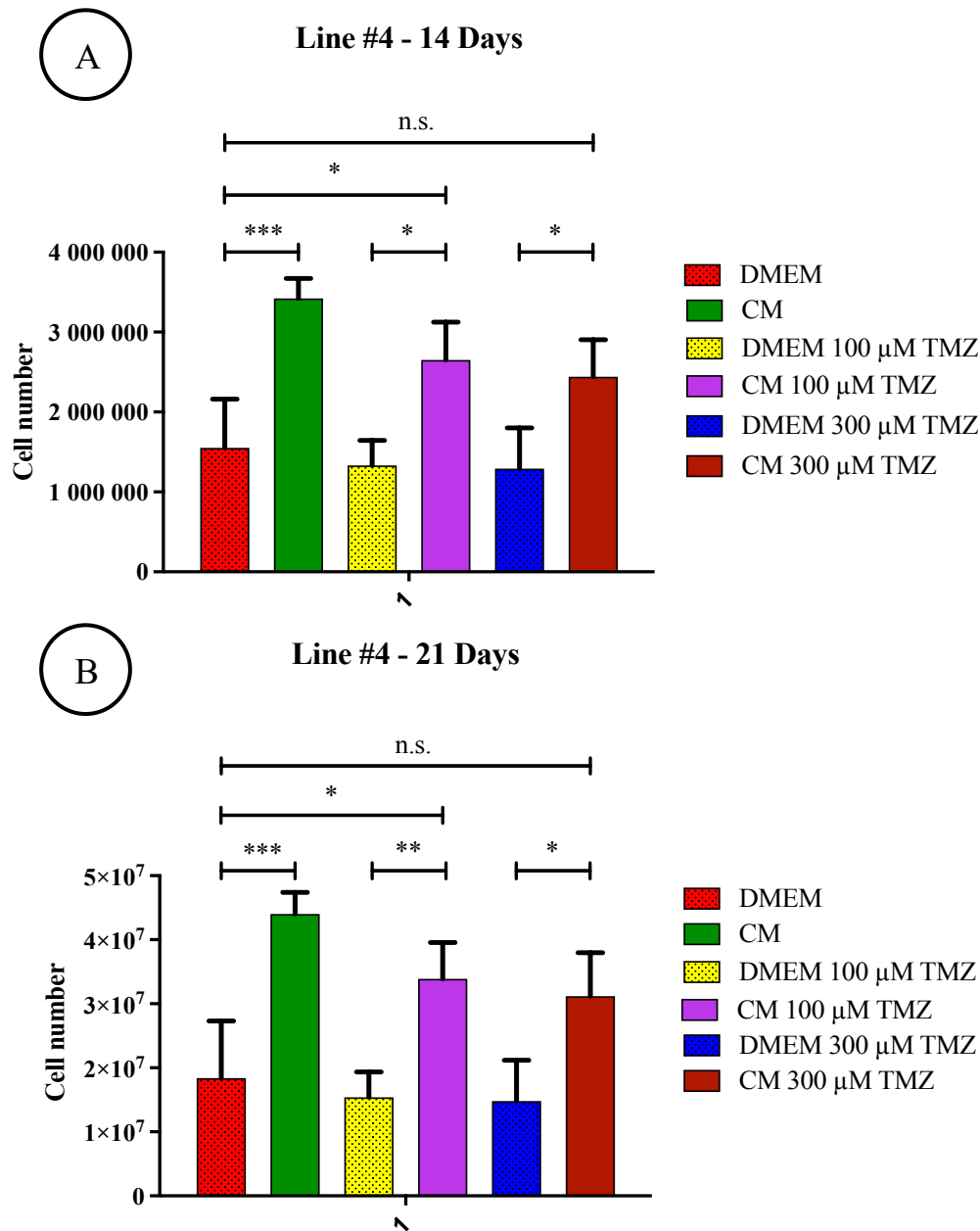


**Figure 12: Serum-free MSCs conditioned medium increases viability of Line #4 GSCs**

The bar charts show the viability measured in cell number of Line #4 on day 14 (A) and on day 21 (B). Every column represents a condition of the mentioned ones on the right. Results are illustrated as the mean  $\pm$  SD. On both days, day 14 and 21, the cell number of the groups CM without TMZ is more than twice as large as the corresponding control group (\*\*\*). Even under conditions of chemotherapy the difference between CM groups with 100 and 300  $\mu$ M and their corresponding DMEM groups with TMZ is considerable on both days. The Y axis represents the cell number in log scale. One-way ANOVA between all groups was performed first (A: P value 0.0004 (\*\*\*); B: P value 0.003 (\*\*\*)). Afterwards, Bonferroni test was carried out in order to compare preselected columns. Statistical significances are indicated in the figure: \*,  $p < 0.05$ ; \*\*,  $p < 0.005$ ; \*\*\*,  $p < 0.0005$ . (n=3)

The bar charts of Figure 12 for Line #4 show comparable results to Line #7 in terms of viability. Again, the CM groups with and without TMZ reveal noticeably higher cell numbers than the corresponding DMEM groups. TMZ doesn't have a significant effect on the cell number in Line #4 when comparing bars in either the DMEM or the CM groups. CM augments cell

numbers irrespective of the presence of TMZ. Consequently, there is no chemoresistance induced by CM for this Line #4.

All in all, conditioned medium increases viability of GSC Line #4. Nevertheless, Line #4 is largely insensitive to TMZ and CM augments cell numbers irrespective of the presence of TMZ. There is no evidence for chemoresistance induced by CM.

To sum up, the proliferation assay illustrates an increase in viability for both GSC lines, Line #7 and Line #4, when incubated with conditioned medium. Nevertheless, there is no evidence for chemoresistance induced by conditioned medium.

In summary, MSCs migrate to invasive areas of glioblastoma. Invasive tumor areas might remain in the brain after surgery and due to a functional blood-brain barrier may represent brain areas not exposed to serum factors. The proliferation assay implies that MSCs act in a pro-tumorigenic manner under the given serum-free circumstances. Considering all the results, this study suggests that MSCs are capable to support tumor relapse formation by inducing viability in glioma cells that remain in the brain after neurosurgical resection.

## 4 Discussion

### 4.1 MSCs tropism for tumors

The experiments of my work show that MSCs migrate to areas where tumor cells reside. Hence, there is evidence of MSCs tropism for tumors. This result is in agreement with the work of Nakamizo et al., who report that MSCs integrate into glioma after intracranial injection or intravascular delivery (83). This tropism might be exploited to therapeutic advantages. In recent years, lots of experiments have been carried out which focused on MSCs as a possible drug carrier (84). For instance, MSCs transfected with tumor necrosis factor-related apoptosis inducing ligand (TRAIL) and injected in the tumor were demonstrated to be therapeutically efficient against glioma (85, 86).

Moreover, MSCs are attracted by other tumor species as well. Kidd et al. analyzed the migration of MSCs expressing firefly luciferase after injecting them both intravenously and intraperitoneally. They found evidence of MSC tropism for tumors like breast or ovarian cancer and for injured tissues, like e.g. wounds (87). Their role in wounds is complex and includes “modulation of tissue inflammation, regulation of cellular proliferation, and differentiation and remodelling of the injured tissue” (48). In patients with severe traumatic injuries, circulating MSCs could be detected as a response to bone fractures (88). They are believed to play an important part in recovery processes (88). In general, tumors can be considered as “wounds that do not heal” (89). This raises many questions about the determinants responsible for the tumor tropism. In their review, Shi et al. mention the chemokines CC-chemokine ligand 2 (CCL2), CCL5, CXC-chemokine ligand 8 (CXCL8), CXCL12 and CXCL16, secreted by tumor cells, immune cells and tumor stromal cells to play important roles in the recruitment of MSCs (48). Furthermore, growth factors such as vascular endothelial growth factor (VEGF), insulin-like growth factor 1 (IGF1), platelet-derived growth factor (PDGF) and basic fibroblast growth factor (bFGF) are believed to attract MSCs (45). Taken together, a lot of different soluble factors are discussed to be responsible for the tumor tropism. These chemo-attracting factors depend on the type of tumor, components of the tumor environment and its immune status (48).

A concern about using MSCs for tumor targeted therapy is the MSCs ability to modulate immune response (48). MSCs are bidirectionally communicating with cells of the innate and the adaptive immune system (48). Through cytokines and chemokines of the CC and CXC groups, tumor associated MSCs are in complex contact with immune cells (48, 64, 90). MSCs

have a potent immunosuppressive effect (91), but under certain conditions paradoxically enhance both the innate and adaptive immune response (48, 60). All the underlying immunoenhancing or suppressing mechanisms need to be figured out before MSCs can be used as potential delivery tools. If not, the therapeutic antitumorigenic effect of the delivered agent must be strong enough to override any protumorigenic potential of the MSCs. First promising experiments have been carried out by Mirzaei and co-workers who applied engineered MSCs in melanoma (92). Furthermore, the TREAT ME1 trial of MSC based tumor therapy has been initiated (93). This phase I/II clinical trial assesses the efficacy of autologous transplantation of genetically engineered MSCs as potential delivery tools for a cell-based gene therapy in patients suffering from gastrointestinal tumors. In fact, phase I could already demonstrate acceptable safety and tolerability in patients treated with modified MSCs (93, 94).

Besides MSCs, neural stem cells (NSC) are also extensively studied to be a potential therapeutic delivery agent. Preliminary work was carried out by Aboody who claimed NSCs tropism for intracranial glioma (95). However, availability of NSCs is limited due to ethical and logistic issues associated with their isolation from human brains. In contrast, MSCs can simply be harvested from the bone marrow, adipose tissue or the umbilical cord (49). Nevertheless, suboptimal in vitro expansion protocols might alter MSC properties, for instance proliferative rate (96) or genetic instability, which in turn raise biosafety issues (97).

## **4.2 Importance of the tumor microenvironment**

There is a body of literature discussing pro- and antitumorigenic effects of MSCs. My data implies that these effects may depend on the exact localization within a tumor. Several recent studies draw our attention to the importance of the tumor microenvironment (TME) when they for instance suggest that the ratio of tumor stromal cells in the tumor mass influences the poor outcome of patients receiving chemotherapy (98, 99). After being recruited to the tumor site, MSCs are closely interrelated with other cell types of the TME. Stromal cells and tumor cells reprogram or educate MSCs through complex mechanisms in many tumors (100), including GBM (73). Many cells of the TME like microglia, macrophages, endothelial cells, astrocytes and interestingly, MSCs are believed to sustain glioblastoma stem cell (GSC) self-renewal (45). Likewise, MSCs have been identified to be involved in angiogenesis by differentiation into pericyte-like cells or secretion of VEGF (101-103). In their analysis Shahar et al. claim that the percentage of glioma associated MSCs inversely correlates with patient survival (104). This means that MSCs promote aggressive behavior of gliomas (104). The in vivo experiments of

my project demonstrate that MSCs are part of the TME, therefore interaction between MSCs, glioma and nonmalignant stromal cells of the TME is very likely to happen. My results not only indicate an indirect interaction between MSCs and GBM cells, but also suggest direct cell to cell interaction.

The in-vitro experiments of my study point out that MSCs as part of the TME have viability increasing effects on GBM. A number of studies have found that MSCs can even induce resistance to chemotherapy to tumor cells in general (105, 106). An in vivo study by Roodhart et al. reveals that after platinum-based chemotherapies, polyunsaturated fatty acids (PUFA) are secreted by MSCs (105). In turn, PUFAs are able to generate resistance to platinum-based therapies in colorectal, lung and breast cancer (105). Another in vitro approach, similar to my experiment, shows that MSCs conditioned supernatant is able to induce chemoresistance in head and neck squamous cell carcinoma cells against paclitaxel treatment (106). This shows that therapeutic targeting of MSCs could improve the response of tumor cells to chemotherapy.

In fact, the TME is already a potential target for promising therapies. For example, the already mentioned VEGF neutralizing antibody bevacizumab inhibits an important key axis between tumor and TME interaction (107). VEGF, a central driver for tumor related angiogenesis, is not only expressed by glioma cells themselves but by MSCs as well (103, 107). Blockade of immune checkpoints is another concept researchers are currently focusing on regarding the interactions between tumors and TME, for example inhibition of cytotoxic T lymphocyte-associated antigen 4 (CTLA-4) with the antibody ipilimumab in malignant melanoma (108). However, ipilimumab is not adapted to glioma therapy.

Histology of TME in glioma is complex, yet it is crucial to investigate and understand the exact composition of the tumor tissue. Obviously, one should consider that different types of tumors differ fundamentally regarding their invasiveness (109, 110). As mentioned above, GBM represents a highly invasive tumor entity. Accordingly, this affects the TME and by this MSCs. My work focuses on the situation in invasive tumor fronts. I am aware of the fact that there is a fluent transition between tumor center, invasive area and the peritumoral region. In the tumor mass we observe uncontrolled proliferation of tumor cells driven by genomic instability, chromosomal alterations and genetic mutations with an abnormal, dysfunctional tumor vasculature (111). More peripherally, the tissue appears less infiltrated by tumor cells until in regions distant from the tumor the histology shows tissue architecture that resembles healthy

brain areas (112). My categorization into invasive tumor parts and tumor center remains rough and a more precise and exact classification could be relevant for further experiments.

As indicated above, patients with GBM undergo maximal surgical resection (32). Unfortunately, it is hardly possible to resect all of the invasively growing tumor cells; therefore cancerous cells remain in the brain (32). The invasive tumor areas I have denominated in my thesis, represent regions that as well can hardly be resected. Neurosurgeons have to strike a balance between removal of as much malignant tissue as possible without harming functional brain parenchyma that lead to worsening or inducing new neurologic deficits (113). Residual tumor cells are the origin of tumor relapse (114) and my *in vivo* experiment strongly associates them with MSCs. This is clinically interesting for new approaches to anticancer treatment, especially after tumor resection. Recent therapeutical strategies include the inhibition of MSC secreted growth factors, which enhance angiogenesis and survival and proliferation of tumor cells (48). Furthermore, MSC-secreted chemokines which promote invasiveness could be neutralized. Another possible aspect lies in the inhibition of molecules that make cancer cells resistant to chemo- or radiotherapy (48). Moreover, MSCs could be used as a possible tracer for remaining cancer cells or to deliver anticancer agents after surgery.

In my *in vivo* experiments a red fluorescent signal, which could not be linked to a cellular structure containing an intact nucleus, could be observed in the invasive tumor areas besides MSCs. A reasonable explanation for this observation is that this red signal indicates the remnants of MSCs, which have died in the tumor core. After cell death the red fluorescent protein might be released and is thus still detectable.

Overall, this shows that MSCs in the tumor core and in the invasive areas have profound differences in turnover with MSCs in the core dying rapidly and MSCs in the invasive zones being more persistent.

### **4.3 Pro- and antitumorigenic effects of MSC**

My experiments demonstrate that under serum-free conditions, MSCs enhance viability of GBM cells. This is consistent with the work of Vieira de Castro et al, who also found an increase in viability of two glioma cell lines when incubated with serum-free MSCs (MSCs from the Wharton's jelly of the umbilical cord) conditioned medium (115). This protumorigenic effect was shown by Ramazan Uyar, a former member of our research group, for several GBM cell lines (74). Interestingly, he also suggests that under serum containing conditions MSCs act contrarily: viability of glioma cell lines is decreased (74). Contrasting results were also obtained

by Bajetto et al. who describe pro and antitumorigenic effects of MSC derived from the umbilical cord (116). They study both direct (cell to cell interaction) and indirect (via soluble secreted factor in a conditioned medium) interaction between GBM and MSCs. Interestingly, indirect interaction causes the protumorigenic effect (116). Subsequent analysis of the CM reveal high levels of components “that are involved in inflammation, angiogenesis, cell migration and proliferation, such as IL-8, GRO, ENA-78 and IL-6” (116). These findings are in line with my in vitro studies working with conditioned medium. In their studies, medium is as well conditioned without serum factors.

In this context, it is interesting to again mention the MSCs role in wound healing processes. They are supposed to coordinate two responses after tissue injury, the immunomodulatory response and the trophic response (59). Damaged tissue most likely includes injured vessels, which in turn leads to leakage of blood-derived molecules (59). These molecules are able to activate inflammatory processes (e.g. attach of pathogens or influence on macrophage function) in MSCs in order to fight potential infections (117). Moreover, MSCs are believed to contribute to damage resolution by supporting a regenerative microenvironment including anti-apoptotic, mitotic, anti-scarring and angiogenic processes (59, 118). These polarizing effects of MSCs in wound healing processes could potentially be transferable to MSCs behavior in tumors. There is a good probability that the proinflammatory response is associated with the antitumorigenic state of MSCs, whereas the trophic response might resemble the protumorigenic behavior of MSCs. I hypothesize that the factors pushing MSCs towards the antitumorigenic or proinflammatory behavior are serum-derived. On the other hand, the serum-free situation should lead to a protumorigenic behavior of MSCs. This I could confirm in my in vitro experimental schedule.

As indicated, a serum-derived factor or a combination of serum-derived factors influence MSCs behavior (74, 115, 119). That underlines the relevance of the dextrane application in my experiment. As already explained, intravenous application of 70 kDa dextrane is a technically appropriate and valuable option of current methods to examine leakage in the brain. In invasive parts of the tumor, where a stable interaction between glioma cells and MSCs takes place, the BBB is largely intact. Consequently, MSCs in invasive tumor areas are not exposed to serum factors larger than 70 kDa. Therefore, it seems likely that factors pushing MSCs towards an antitumorigenic behavior might be serum-derived and more than 70 kDa large. However, it is not possible to rule out that leakiness of smaller molecules than 70 kDa may occur.

MSC cultures are able to undergo multilineage differentiation in vitro depending on the medium composition in which they reside (45). Distinct circumstances determine their transformation to diverging progeny with different cell characteristics. This differentiation potential ranges from chondrogenic, osteogenic and adipogenic under standard protocols, over myogenic to even cardiomyogenic and hepatogenic (45). Cellular heterogeneity and varying differentiation capacity hamper the translatability of in vitro biological features into in vivo effects (45).

The present in vitro studies have investigated in two GBM cell lines. Line #4 represents a classical subtype and line #7 is defined as proneural. Consequently, it might be interesting to examine mesenchymal GBM lines in order to reveal if the same findings can be achieved.

#### **4.4 Reciprocal interactions between MSCs and glioma cells**

Initially, MSCs get recruited, activated and educated by the tumor, the TME or both (66, 120). Recent evidence suggests that MSCs are either attracted from local brain sites or the bone marrow (66, 120). In response to the physiological matrix they are confronted with and depending on their type and original source, MSCs release factors that in turn alternately affect tumor cells, the TME or both (45). Likewise, my studies highlight recruitment of MSCs to invasive parts of glioma and provide further evidence for protumorigenic effects of MSCs under serum-free conditions. MSC and GBM cells interact directly but potentially contact-free by paracrine effects, extracellular vesicles or miRNA (45). It has now even been hypothesized that MSCs and GBM cells are able to fuse, thereby promoting neovascularization (121). The in vitro experiments I carried out investigate the interactions via MSCs released factors. They point out the protumorigenic effect of MSCs on GBM under certain circumstances (without serum factors). It is discussed that MSCs exert their impact mainly through their secretory function (122). Hence, experiments conducted with conditioned medium or supernatant seem quite reasonable in order to analyze interaction between GBM and MSCs. These experiments also consider factors like extracellular vesicles or miRNA secreted by MSCs, which have proven to have effects on different types of glioblastoma (123, 124). Interestingly, cell communication between MSCs and glioma cells is bidirectional via extracellular vesicles: glioma is able to induce a tumor-like phenotype in mesenchymal stem cells which promotes their invasion and migration (125). This implies that in addition to recruitment to tumors, GBM cells trigger further cell processes in MSCs, most of them having probably not even been discovered yet. Interestingly, experiments conducted by Uyar showed that prior challenge of MSC with GBM-CM did not change the tumor supportive effect of MSC-CM (74).



#### **4.5 Perspective of MSC-based therapy for GBM**

In recent years, MSCs have gained much attention as a potential objective for innovative therapeutical ideas in glioma (45). Pathways leading to protumorigenic effects of MSCs could be inhibited, whereas mechanisms that induce MSCs antitumorigenic behavior could be enhanced or facilitated. Another target might be MSC's influence on therapy resistance, for instance chemo- and radiotherapy. Key pathways between MSC and GBM cells that induce resistance in cancer cells could be suppressed. However, inconsistent results provoked controversial debates about MSCs potential in glioma (45). Complications like MSC tissue source, isolation and culture protocols, tumor type, administration route and timing might have led to contrasting observations. In depth analysis of the underlying interactions between GBM cells and MSCs, standardization of methods and a better exchange of information among research groups are pivotal for a future evaluation of MSC-based therapy (45).

MSCs migratory capacity to tumor sites might be exploited in different approaches. In order to track down GBM cells, before and after surgery, specifically labeled MSCs could be used as in vivo tracer (126). Another interesting potential lies in genetically engineered MSCs delivering cytotoxic agents, for example paclitaxel (127). MSCs transfected to express proapoptotic factors (86) or oncolytic viruses (128) have also been discussed to be effective in glioma. Furthermore, promising approaches have developed recently utilizing transfected MSCs to secrete miRNA loaded exosomes with antitumorigenic potential in GBM. For instance, intracranially injected MSCs that release exosomes carrying miR-124a lead to decreased cell proliferation and migration and moreover, enhance chemosensitivity (129-131).

These strategies converting MSCs into therapeutical vehicles to migrate to tumors and release antitumoral agents are encouraging, but still caution must be taken due to potential negative unintended side effects of MSCs.

To sum up, I found that MSCs migrate to invasive parts of the tumor, which provides further evidence of MSCs tropism for tumor cells. In the tumor center MSCs may accumulate but appear to have a short half live, as no MSCs could be detected in the tumor center in my experimental schedule. MSCs may be pathologically important in the main tumor mass, but this mass is neurosurgically resected. However, invasive tumor areas remain after surgery and due to a functional blood-brain barrier may represent brain areas not exposed to serum-derived factors. In my in vitro experiments I aimed to model this pathologically relevant aspect of MSC/GBM interaction under simplified serum-free conditions. In order to generate conditioned medium, MSCs were cultivated without serum factors and the medium was harvested after 72

hours. The viability in two lines of GSCs was enhanced when they were incubated with mesenchymal stem cells conditioned medium even under conditions of chemotherapy. Future studies should investigate in the mechanisms behind the tumor-supportive effects of MSCs in order to inhibit or target underlying pro-proliferative signaling processes.

## 5 Conclusion

Among other cell lines of the tumor microenvironment, mesenchymal stem cells play an important role in glioma progression. However, many diverging aspects were shown about the complex interaction between mesenchymal stem cells and tumor cells. This study aimed to model one pathologically relevant aspect of the *in vivo* interaction between mesenchymal stem cells and glioma cells under simplified *in vitro* conditions in order to analyze a potential effect on the viability of glioma cells.

First, mice were intracranially inoculated with glioma cells. Once the tumor reached a detectable size, mesenchymal stem cells were injected into the brain into the main tumor mass. After sacrificing the mice, brain slice sections were analyzed with regards to the mesenchymal stem cells location and blood-brain barrier integrity in glioma. Furthermore, a cell counting assay was performed studying glioma cells viability under serum-free mesenchymal stem cell conditioned medium. The reason is that mesenchymal stem cells may be controlled by injury contact when exposed to blood serum-derived factors: They coordinate acute inflammatory injury responses in situation of damage and may contribute to damage-resolution later by supporting tissue healing and regeneration.

The *in vivo* experiment shows migration of mesenchymal stem cells to invasive parts of the tumor. It was demonstrated that in these regions the blood-brain barrier is widely intact. Hence, serum-derived factors larger than the size of 70 kDa do not reach the structures where mesenchymal stem cells reside. Consequently, this serum-free situation was modeled in an *in vitro* proliferation assay. Serum-free medium, which was conditioned by mesenchymal stem cells, enhances viability in two lines of glioma stem cells even under conditions of chemotherapy.

This paper adds to our understanding of the complex interaction between mesenchymal stem cells and glioma cells. The results of the study provide evidence for mesenchymal stem cells tropism for invasive regions of glioblastoma. These invasive regions remain in the brain after neurosurgery, representing the source of tumor relapse. Taken together, these encouraging results suggest that mesenchymal stem cells are able to support tumor relapse formation by improving viability of glioma cells even under conditions of chemotherapy. This makes mesenchymal stem cells and their interaction with glioblastoma promising potential therapeutical targets to evaluate in glioblastoma therapy in the future.

## List of references

1. Quinn T Ostrom GC, Haley Gittleman, Nirav Patil, Kristin Waite, Carol Kruchko, Jill S Barnholtz-Sloan CBTRUS Statistical Report: Primary Brain and Other Central Nervous System Tumors Diagnosed in the United States in 2012–2016. *Neuro Oncol.* 2019;21:1-100.
2. Marenco-Hillebrand L WO, Suarez-Meade P, Mampre D, Jackson C, Peterson J, Trifiletti D, Hammack J, Ortiz K, Lesser E, Spiegel M, Prevatt C, Hawayek M, Quinones-Hinojosa A, Chaichana<sup>9</sup>. Trends in glioblastoma: outcomes over time and type of intervention: a systematic evidence based analysis. *Neuro Oncol.* 2020(147):297-307.
3. Lim DA, Cha S, Mayo MC, Chen M-H, Keles E, VandenBerg S, et al. Relationship of glioblastoma multiforme to neural stem cell regions predicts invasive and multifocal tumor phenotype. *Neuro Oncol.* 2007;9(4):424-9.
4. Ohgaki H, Kleihues P. Genetic Pathways to Primary and Secondary Glioblastoma. *The American Journal of Pathology.* 2007;170(5):1445-53.
5. Louis DN, Perry, A., Reifenberger, G. et al. The 2016 World Health Organization Classification of Tumors of the Central Nervous System: a summary. *Acta Neuropathol.* 2016;131:803-20.
6. Louis DN HE, Cairncross JG. Glioma classification: A molecular Reappraisal. *The American Journal of Pathology.* 2001;159(3):779-86.
7. Verhaak RGW, Hoadley KA, Purdom E, Wang V, Qi Y, Wilkerson MD, et al. Integrated genomic analysis identifies clinically relevant subtypes of glioblastoma characterized by abnormalities in PDGFRA, IDH1, EGFR, and NF1. *Cancer Cell.* 2010;17(1):98-110.
8. Bondy ML, Scheurer ME, Malmer B, Barnholtz-Sloan JS, Davis FG, Il'yasova D, et al. Brain tumor epidemiology: Consensus from the Brain Tumor Epidemiology Consortium. *Cancer.* 2008;113(S7):1953-68.
9. Quinn T. Ostrom GC, Haley Gittleman, Nirav Patil, Kristin Waite, Carol Kruchko, Jill S Barnholtz-Sloan CBTRUS Statistical Report: Primary Brain and Other Central Nervous System Tumors Diagnosed in the United States in 2012–2016. *Neuro-Oncology.* 2019;21:1-100.
10. Thakkar JP DT, Horbinski C, Ostrom QT, Lightner DD, Barnholtz-Sloan JS, Villano JL. Epidemiologic and Molecular Prognostic Review of Glioblastoma. *American Association for Cancer Research.* 2014;23(10):1985-96.
11. Kinnersley B, Labussière M, Holroyd A, Di Stefano A-L, Broderick P, Vijayakrishnan J, et al. Genome-wide association study identifies multiple susceptibility loci for glioma. *Nature Communications.* 2015;6(1):8559.
12. Scheurer ME, Amirian ES, Davlin SL, Rice T, Wrensch M, Bondy ML. Effects of antihistamine and anti-inflammatory medication use on risk of specific glioma histologies. *International Journal of Cancer.* 2011;129(9):2290-6.

13. Hur H, Jung S, Jung T-Y, Kim I-Y. Cerebellar glioblastoma multiforme in an adult. *J Korean Neurosurg Soc.* 2008;43(4):194-7.
14. Hsu E, Keene D, Ventureyra E, Matzinger MA, Jimenez C, Wang HS, et al. Bone marrow metastasis in astrocytic gliomata. *Journal of Neuro-Oncology.* 1998;37(3):285-93.
15. Hanif F, Muzaffar K, Perveen K, Malhi SM, Simjee SU. Glioblastoma Multiforme: A Review of its Epidemiology and Pathogenesis through Clinical Presentation and Treatment. *Asian Pac J Cancer Prev.* 2017;18(1):3-9.
16. Aldape K, Zadeh G, Mansouri S, Reifenberger G, von Deimling A. Glioblastoma: pathology, molecular mechanisms and markers. *Acta Neuropathologica.* 2015;129(6):829-48.
17. Kleihues P, Ohgaki H. Phenotype vs Genotype in the Evolution of Astrocytic Brain Tumors. *Toxicologic Pathology.* 2000;28(1):164-70.
18. Agnihotri S, Burrell KE, Wolf A, Jalali S, Hawkins C, Rutka JT, et al. Glioblastoma, a Brief Review of History, Molecular Genetics, Animal Models and Novel Therapeutic Strategies. *Archivum Immunologiae et Therapiae Experimentalis.* 2013;61(1):25-41.
19. Gladson CL, Prayson RA, Liu WM. The pathobiology of glioma tumors. *Annu Rev Pathol.* 2010;5:33-50.
20. Cancer Genome Atlas Research N. Comprehensive genomic characterization defines human glioblastoma genes and core pathways. *Nature.* 2008;455(7216):1061-8.
21. Nørøxe DS, Poulsen HS, Lassen U. Hallmarks of glioblastoma: a systematic review. *ESMO Open.* 2017;1(6):e000144-e.
22. Böglér O, Su Huang HJ, Kleihues P, Cavenee WK. The p53 gene and its role in human brain tumors. *Glia.* 1995;15(3):308-27.
23. Osanai T, Takagi Y, Toriya Y, Nakagawa T, Aruga T, Iida S, et al. Inverse Correlation Between the Expression of O6-Methylguanine-DNA Methyl Transferase (MGMT) and p53 in Breast Cancer. *Japanese Journal of Clinical Oncology.* 2005;35(3):121-5.
24. Fujisawa H, Reis RM, Nakamura M, Colella S, Yonekawa Y, Kleihues P, et al. Loss of Heterozygosity on Chromosome 10 Is More Extensive in Primary (De Novo) Than in Secondary Glioblastomas. *Laboratory Investigation.* 2000;80(1):65-72.
25. Hegi ME, Diserens A-C, Gorlia T, Hamou M-F, de Tribolet N, Weller M, et al. MGMT Gene Silencing and Benefit from Temozolomide in Glioblastoma. *New England Journal of Medicine.* 2005;352(10):997-1003.
26. Ohgaki H, Dessen P, Jourde B, Horstmann S, Nishikawa T, Di Patre P-L, et al. Genetic Pathways to Glioblastoma. A Population-Based Study. 2004;64(19):6892-9.
27. Omuro A, DeAngelis LM. Glioblastoma and Other Malignant Gliomas: A Clinical Review. *JAMA.* 2013;310(17):1842-50.
28. Posti JP, Bori M, Kauko T, Sankinen M, Nordberg J, Rahi M, et al. Presenting symptoms of glioma in adults. *Acta Neurologica Scandinavica.* 2015;131(2):88-93.

29. Shukla G, Alexander GS, Bakas S, Nikam R, Talekar K, Palmer JD, et al. Advanced magnetic resonance imaging in glioblastoma: a review. *Chin Clin Oncol*. 2017;6(4):40.
30. Abd-Elghany AA, Naji AA, Alonazi B, Aldosary H, Alsufayan MA, Alnasser M, et al. Radiological characteristics of glioblastoma multiforme using CT and MRI examination. *Journal of Radiation Research and Applied Sciences*. 2019;12(1):289-93.
31. Nelson S, Cha, Soonmee. Imaging Glioblastoma Multiforme. *Cancer J*. 2003;9(2):134-145. Cited in: Journals@Ovid Full Text at <http://ovidsp.ovid.com/ovidweb.cgi?T=JS&PAGE=reference&D=ovftf&NEWS=N&AN=00130404-200303000-00009>. Accessed May 09, 2020. Imaging Glioblastoma Multiforme. . *Cancer Journal*. 2003;9(2):134-45.
32. Iacob G, Dinca EB. Current data and strategy in glioblastoma multiforme. *J Med Life*. 2009;2(4):386-93.
33. Vignard J, Mirey G, Salles B. Ionizing-radiation induced DNA double-strand breaks: A direct and indirect lighting up. *Radiotherapy and Oncology*. 2013;108(3):362-9.
34. Stupp R, Mason WP, van den Bent MJ, Weller M, Fisher B, Taphoorn MJ, et al. Radiotherapy plus concomitant and adjuvant temozolomide for glioblastoma. *N Engl J Med*. 2005;352(10):987-96.
35. Herrlinger U, Tzaridis T, Mack F, Steinbach JP, Schlegel U, Sabel M, et al. Lomustine-temozolomide combination therapy versus standard temozolomide therapy in patients with newly diagnosed glioblastoma with methylated MGMT promoter (CeTeG/NOA-09): a randomised, open-label, phase 3 trial. *Lancet*. 2019;393(10172):678-88.
36. Karachi A, Dastmalchi F, Mitchell DA, Rahman M. Temozolomide for immunomodulation in the treatment of glioblastoma. *Neuro Oncol*. 2018;20(12):1566-72.
37. Grossman SA, Ye X, Lesser G, Sloan A, Carraway H, Desideri S, et al. Immunosuppression in patients with high-grade gliomas treated with radiation and temozolomide. *Clin Cancer Res*. 2011;17(16):5473-80.
38. Chinot OL, Wick W, Mason W, Henriksson R, Saran F, Nishikawa R, et al. Bevacizumab plus radiotherapy-temozolomide for newly diagnosed glioblastoma. *N Engl J Med*. 2014;370(8):709-22.
39. Khasraw M, Ameratunga MS, Grant R, Wheeler H, Pavlakis N. Antiangiogenic therapy for high-grade glioma. *Cochrane Database Syst Rev*. 2014(9):Cd008218.
40. Wong ET, Swanson KD. Dexamethasone—Friend or Foe for Patients With Glioblastoma? *JAMA Neurology*. 2019;76(3):247-8.
41. Rosati A, Buttolo L, Stefini R, Todeschini A, Cenzato M, Padovani A. Efficacy and safety of levetiracetam in patients with glioma: a clinical prospective study. *Arch Neurol*. 2010;67(3):343-6.
42. Hesketh PJ, Kris MG, Basch E, Bohlke K, Barbour SY, Clark-Snow RA, et al. Antiemetics: American Society of Clinical Oncology Clinical Practice Guideline Update. *J Clin Oncol*. 2017;35(28):3240-61.

43. De Vleeschouwer S, Bergers G. Glioblastoma: To Target the Tumor Cell or the Microenvironment? In: De Vleeschouwer S, editor. Glioblastoma. Brisbane (AU): Codon Publications  
Copyright: The Authors.; 2017.
44. Klemm F, Joyce JA. Microenvironmental regulation of therapeutic response in cancer. *Trends Cell Biol.* 2015;25(4):198-213.
45. Bajetto A, Thellung S, Dellacasagrande I, Pagano A, Barbieri F, Florio T. Cross talk between mesenchymal and glioblastoma stem cells: Communication beyond controversies. *STEM CELLS Translational Medicine.* 2020;9(11):1310-30.
46. Pittenger MF, Discher DE, Péault BM, Phinney DG, Hare JM, Caplan AI. Mesenchymal stem cell perspective: cell biology to clinical progress. *npj Regenerative Medicine.* 2019;4(1):22.
47. Friedenstein AJ, Chailakhjan RK, Lalykina KS. The development of fibroblast colonies in monolayer cultures of guinea-pig bone marrow and spleen cells. *Cell Tissue Kinet.* 1970;3(4):393-403.
48. Shi Y, Du L, Lin L, Wang Y. Tumour-associated mesenchymal stem/stromal cells: emerging therapeutic targets. *Nature Reviews Drug Discovery.* 2017;16(1):35-52.
49. Uccelli A, Moretta L, Pistoia V. Mesenchymal stem cells in health and disease. *Nat Rev Immunol.* 2008;8(9):726-36.
50. Zhou BO, Yue R, Murphy MM, Peyer JG, Morrison SJ. Leptin-receptor-expressing mesenchymal stromal cells represent the main source of bone formed by adult bone marrow. *Cell Stem Cell.* 2014;15(2):154-68.
51. Dominici M, Le Blanc K, Mueller I, Slaper-Cortenbach I, Marini F, Krause D, et al. Minimal criteria for defining multipotent mesenchymal stromal cells. The International Society for Cellular Therapy position statement. *Cytotherapy.* 2006;8(4):315-7.
52. Kern S, Eichler H, Stoeve J, Klüter H, Bieback K. Comparative Analysis of Mesenchymal Stem Cells from Bone Marrow, Umbilical Cord Blood, or Adipose Tissue. *Stem Cells.* 2006;24(5):1294-301.
53. Lv F-J, Tuan RS, Cheung KMC, Leung VYL. Concise Review: The Surface Markers and Identity of Human Mesenchymal Stem Cells. *Stem Cells.* 2014;32(6):1408-19.
54. Batouli S, Miura M, Brahim J, Tsutsui TW, Fisher LW, Gronthos S, et al. Comparison of Stem-cell-mediated Osteogenesis and Dentinogenesis. *Journal of Dental Research.* 2003;82(12):976-81.
55. Wilson A, Trumpp A. Bone-marrow haematopoietic-stem-cell niches. *Nature Reviews Immunology.* 2006;6(2):93-106.
56. Paul G, Özen I, Christophersen NS, Reinbothe T, Bengzon J, Visse E, et al. The Adult Human Brain Harbors Multipotent Perivascular Mesenchymal Stem Cells. *PLOS ONE.* 2012;7(4):e35577.

57. Lojewski X, Srimasorn S, Rauh J, Francke S, Wobus M, Taylor V, et al. Perivascular Mesenchymal Stem Cells From the Adult Human Brain Harbor No Intrinsic Neuroectodermal but High Mesodermal Differentiation Potential. *STEM CELLS Translational Medicine*. 2015;4(10):1223-33.
58. Crisan M, Yap S, Casteilla L, Chen C-W, Corselli M, Park TS, et al. A Perivascular Origin for Mesenchymal Stem Cells in Multiple Human Organs. *Cell Stem Cell*. 2008;3(3):301-13.
59. Caplan AI, Correa D. The MSC: an injury drugstore. *Cell Stem Cell*. 2011;9(1):11-5.
60. Wang Y, Chen X, Cao W, Shi Y. Plasticity of mesenchymal stem cells in immunomodulation: pathological and therapeutic implications. *Nat Immunol*. 2014;15(11):1009-16.
61. Vojtassák J, Danisovic L, Kubes M, Bakos D, Jarábek L, Ulicná M, et al. Autologous biograft and mesenchymal stem cells in treatment of the diabetic foot. *Neuro Endocrinol Lett*. 2006;27 Suppl 2:134-7.
62. Zhang Z, Lin H, Shi M, Xu R, Fu J, Lv J, et al. Human umbilical cord mesenchymal stem cells improve liver function and ascites in decompensated liver cirrhosis patients. *J Gastroenterol Hepatol*. 2012;27 Suppl 2:112-20.
63. Sun L, Wang D, Liang J, Zhang H, Feng X, Wang H, et al. Umbilical cord mesenchymal stem cell transplantation in severe and refractory systemic lupus erythematosus. *Arthritis Rheum*. 2010;62(8):2467-75.
64. Ren G, Zhao X, Wang Y, Zhang X, Chen X, Xu C, et al. CCR2-dependent recruitment of macrophages by tumor-educated mesenchymal stromal cells promotes tumor development and is mimicked by TNF $\alpha$ . *Cell Stem Cell*. 2012;11(6):812-24.
65. Thomas JG, Kerrigan BCP, Hossain A, Gumin J, Shinojima N, Nwajei F, et al. Ionizing radiation augments glioma tropism of mesenchymal stem cells. *Journal of neurosurgery*. 2017;128(1):287-95.
66. Behnan J, Isakson P, Joel M, Cilio C, Langmoen IA, Vik - Mo EO, et al. Recruited brain tumor - derived mesenchymal stem cells contribute to brain tumor progression. *Stem Cells*. 2014;32(5):1110-23.
67. Menon LG, Pratt J, Yang HW, Black PM, Sorensen GA, Carroll RS. Imaging of human mesenchymal stromal cells: homing to human brain tumors. *Journal of Neuro-Oncology*. 2012;107(2):257-67.
68. Cao M, Mao J, Duan X, Lu L, Zhang F, Lin B, et al. In vivo tracking of the tropism of mesenchymal stem cells to malignant gliomas using reporter gene - based MR imaging. *International Journal of Cancer*. 2018;142(5):1033-46.
69. Qiao Y, Gumin J, MacLellan CJ, Gao F, Bouchard R, Lang FF, et al. Magnetic resonance and photoacoustic imaging of brain tumor mediated by mesenchymal stem cell labeled with multifunctional nanoparticle introduced via carotid artery injection. *Nanotechnology*. 2018;29(16):165101.



70. Liu L, Eckert MA, Riazifar H, Kang D-K, Agalliu D, Zhao W. From Blood to the Brain: Can Systemically Transplanted Mesenchymal Stem Cells Cross the Blood-Brain Barrier? *Stem Cells International*. 2013;2013:435093.
71. Clinical Trials: US National Institute of Health; 2021 [cited 2021 6th December]. Available from: <https://ClinicalTrials.gov>.
72. Egeblad M, Nakasone ES, Werb Z. Tumors as Organs: Complex Tissues that Interface with the Entire Organism. *Developmental Cell*. 2010;18(6):884-901.
73. Hossain A, Gumin J, Gao F, Figueroa J, Shinojima N, Takezaki T, et al. Mesenchymal Stem Cells Isolated From Human Gliomas Increase Proliferation and Maintain Stemness of Glioma Stem Cells Through the IL-6/gp130/STAT3 Pathway. *Stem Cells*. 2015;33(8):2400-15.
74. Uyar R. Glioma-associated mesenchymal stem cells have profound effects on brain tumors. München: Ludwig Maximilians Universität München; 2019.
75. Galli R, Binda E, Orfanelli U, Cipelletti B, Gritti A, De Vitis S, et al. Isolation and characterization of tumorigenic, stem-like neural precursors from human glioblastoma. *Cancer Res*. 2004;64(19):7011-21.
76. Stem-cell-technologiesTM. AccutaseTM - Product description: Stem cell TechnologiesTM; 2021 [Available from: [https://cdn.stemcell.com/media/files/pis/29637-PIS\\_1\\_1\\_0.pdf?\\_ga=2.28300798.377206543.1620980337-240858722.1620980336](https://cdn.stemcell.com/media/files/pis/29637-PIS_1_1_0.pdf?_ga=2.28300798.377206543.1620980337-240858722.1620980336)].
77. Horwitz EM, Le Blanc K, Dominici M, Mueller I, Slaper-Cortenbach I, Marini FC, et al. Clarification of the nomenclature for MSC: The International Society for Cellular Therapy position statement. *Cytotherapy*. 2005;7(5):393-5.
78. Masters JR, Stacey GN. Changing medium and passaging cell lines. *Nature Protocols*. 2007;2(9):2276-84.
79. Thalmeier K, Meissner P, Reisbach G, Falk M, Brechtel A, Dörmer P. Establishment of two permanent human bone marrow stromal cell lines with long-term post irradiation feeder capacity. *Blood*. 1994;83(7):1799-807.
80. Egawa G, Nakamizo S, Natsuaki Y, Doi H, Miyachi Y, Kabashima K. Intravital analysis of vascular permeability in mice using two-photon microscopy. *Sci Rep*. 2013;3:1932-.
81. Natarajan R, Northrop N, Yamamoto B. Fluorescein Isothiocyanate (FITC)-Dextran Extravasation as a Measure of Blood-Brain Barrier Permeability. *Curr Protoc Neurosci*. 2017;79:9.58.1-9.15.
82. Solár P, Zamani A, Kubičková L, Dubový P, Joukal M. Choroid plexus and the blood-cerebrospinal fluid barrier in disease. *Fluids and Barriers of the CNS*. 2020;17(1):35.
83. Nakamizo A, Marini F, Amano T, Khan A, Studeny M, Gumin J, et al. Human Bone Marrow-Derived Mesenchymal Stem Cells in the Treatment of Gliomas. *Cancer Research*. 2005;65(8):3307-18.

84. Hu YL, Fu YH, Tabata Y, Gao JQ. Mesenchymal stem cells: a promising targeted-delivery vehicle in cancer gene therapy. *J Control Release*. 2010;147(2):154-62.
85. Kim SM, Lim JY, Park SI, Jeong CH, Oh JH, Jeong M, et al. Gene Therapy Using TRAIL-Secreting Human Umbilical Cord Blood-Derived Mesenchymal Stem Cells against Intracranial Glioma. *Cancer Research*. 2008;68(23):9614-23.
86. Choi SA, Hwang S-K, Wang K-C, Cho B-K, Phi JH, Lee JY, et al. Therapeutic efficacy and safety of TRAIL-producing human adipose tissue-derived mesenchymal stem cells against experimental brainstem glioma. *Neuro Oncol*. 2011;13(1):61-9.
87. Kidd S, Spaeth E, Dembinski JL, Dietrich M, Watson K, Klopp A, et al. Direct evidence of mesenchymal stem cell tropism for tumor and wounding microenvironments using in vivo bioluminescent imaging. *Stem Cells*. 2009;27(10):2614-23.
88. Alm JJ, Koivu HM, Heino TJ, Hentunen TA, Laitinen S, Aro HT. Circulating plastic adherent mesenchymal stem cells in aged hip fracture patients. *J Orthop Res*. 2010;28(12):1634-42.
89. Dvorak HF. Tumors: wounds that do not heal-redux. *Cancer Immunol Res*. 2015;3(1):1-11.
90. Koh BI, Kang Y. The pro-metastatic role of bone marrow-derived cells: a focus on MSCs and regulatory T cells. *EMBO Rep*. 2012;13(5):412-22.
91. Ren G, Zhang L, Zhao X, Xu G, Zhang Y, Roberts AI, et al. Mesenchymal Stem Cell-Mediated Immunosuppression Occurs via Concerted Action of Chemokines and Nitric Oxide. *Cell Stem Cell*. 2008;2(2):141-50.
92. Mirzaei H, Sahebkar A, Avan A, Jaafari MR, Salehi R, Salehi H, et al. Application of Mesenchymal Stem Cells in Melanoma: A Potential Therapeutic Strategy for Delivery of Targeted Agents. *Curr Med Chem*. 2016;23(5):455-63.
93. Niess H, von Einem JC, Thomas MN, Michl M, Angele MK, Huss R, et al. Treatment of advanced gastrointestinal tumors with genetically modified autologous mesenchymal stromal cells (TREAT-ME1): study protocol of a phase I/II clinical trial. *BMC Cancer*. 2015;15:237.
94. von Einem JC, Peter S, Günther C, Volk H-D, Grütz G, Salat C, et al. Treatment of advanced gastrointestinal cancer with genetically modified autologous mesenchymal stem cells - TREAT-ME-1 - a phase I, first in human, first in class trial. *Oncotarget*. 2017;8(46):80156-66.
95. Aboody KS, Brown A, Rainov NG, Bower KA, Liu S, Yang W, et al. Neural stem cells display extensive tropism for pathology in adult brain: Evidence from intracranial gliomas. *Proceedings of the National Academy of Sciences*. 2000;97(23):12846-51.
96. Baxter MA, Wynn RF, Jowitt SN, Wraith JE, Fairbairn LJ, Bellantuono I. Study of Telomere Length Reveals Rapid Aging of Human Marrow Stromal Cells following In Vitro Expansion. *Stem Cells*. 2004;22(5):675-82.

97. Neri S. Genetic Stability of Mesenchymal Stromal Cells for Regenerative Medicine Applications: A Fundamental Biosafety Aspect. *International Journal of Molecular Sciences*. 2019;20(10):2406.
98. Bissell MJ, Labarge MA. Context, tissue plasticity, and cancer: are tumor stem cells also regulated by the microenvironment? *Cancer Cell*. 2005;7(1):17-23.
99. Huijbers A, Tollenaar RA, v Pelt GW, Zeestraten EC, Dutton S, McConkey CC, et al. The proportion of tumor-stroma as a strong prognosticator for stage II and III colon cancer patients: validation in the VICTOR trial. *Ann Oncol*. 2013;24(1):179-85.
100. Berger L, Shamai Y, Skorecki KL, Tzukerman M. Tumor Specific Recruitment and Reprogramming of Mesenchymal Stem Cells in Tumorigenesis. *Stem Cells*. 2016;34(4):1011-26.
101. Yi D, Xiang W, Zhang Q, Cen Y, Su Q, Zhang F, et al. Human Glioblastoma-Derived Mesenchymal Stem Cell to Pericytes Transition and Angiogenic Capacity in Glioblastoma Microenvironment. *Cell Physiol Biochem*. 2018;46(1):279-90.
102. Birnbaum T, Hildebrandt J, Nuebling G, Sostak P, Straube A. Glioblastoma-dependent differentiation and angiogenic potential of human mesenchymal stem cells in vitro. *Journal of Neuro-Oncology*. 2011;105(1):57-65.
103. Beckermann BM, Kallifatidis G, Groth A, Frommhold D, Apel A, Mattern J, et al. VEGF expression by mesenchymal stem cells contributes to angiogenesis in pancreatic carcinoma. *Br J Cancer*. 2008;99(4):622-31.
104. Shahar T, Rozovski U, Hess KR, Hossain A, Gumin J, Gao F, et al. Percentage of mesenchymal stem cells in high-grade glioma tumor samples correlates with patient survival. *Neuro Oncol*. 2016;19(5):660-8.
105. Roodhart JM, Daenen LG, Stigter EC, Prins HJ, Gerrits J, Houthuijzen JM, et al. Mesenchymal stem cells induce resistance to chemotherapy through the release of platinum-induced fatty acids. *Cancer Cell*. 2011;20(3):370-83.
106. Scherzed A, Hackenberg S, Froelich K, Kessler M, Koehler C, Hagen R, et al. BMSC enhance the survival of paclitaxel treated squamous cell carcinoma cells in vitro. *Cancer Biology & Therapy*. 2011;11(3):349-57.
107. Presta LG, Chen H, O'Connor SJ, Chisholm V, Meng YG, Krummen L, et al. Humanization of an Anti-Vascular Endothelial Growth Factor Monoclonal Antibody for the Therapy of Solid Tumors and Other Disorders. *Cancer Research*. 1997;57(20):4593-9.
108. Hodi FS, O'Day SJ, McDermott DF, Weber RW, Sosman JA, Haanen JB, et al. Improved survival with ipilimumab in patients with metastatic melanoma. *N Engl J Med*. 2010;363(8):711-23.
109. Hatoum A, Mohammed R, Zakieh O. The unique invasiveness of glioblastoma and possible drug targets on extracellular matrix. *Cancer Manag Res*. 2019;11:1843-55.
110. Backer-Grøndahl T, Moen BH, Torp SH. The histopathological spectrum of human meningiomas. *Int J Clin Exp Pathol*. 2012;5(3):231-42.

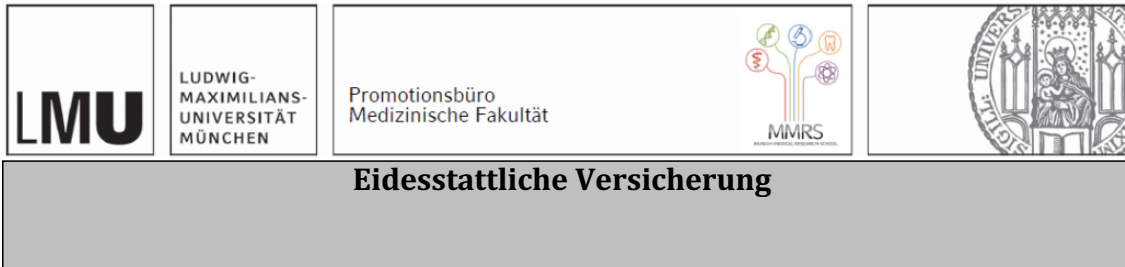
111. Hanahan D, Weinberg RA. Hallmarks of cancer: the next generation. *Cell*. 2011;144(5):646-74.
112. Lemée J-M, Clavreul A, Menei P. Intratumoral heterogeneity in glioblastoma: don't forget the peritumoral brain zone. *Neuro Oncol*. 2015;17(10):1322-32.
113. Yong RL, Lonser RR. Surgery for glioblastoma multiforme: striking a balance. *World Neurosurg*. 2011;76(6):528-30.
114. Hegde GV, de la Cruz C, Eastham-Anderson J, Zheng Y, Sweet-Cordero EA, Jackson EL. Residual tumor cells that drive disease relapse after chemotherapy do not have enhanced tumor initiating capacity. *PloS one*. 2012;7(10):e45647-e.
115. Vieira de Castro J, Gomes ED, Granja S, Anjo SI, Baltazar F, Manadas B, et al. Impact of mesenchymal stem cells' secretome on glioblastoma pathophysiology. *Journal of Translational Medicine*. 2017;15(1):200.
116. Bajetto A, Pattarozzi A, Corsaro A, Barbieri F, Daga A, Bosio A, et al. Different Effects of Human Umbilical Cord Mesenchymal Stem Cells on Glioblastoma Stem Cells by Direct Cell Interaction or Via Released Soluble Factors. *Frontiers in Cellular Neuroscience*. 2017;11(312).
117. Bernardo Maria E, Fibbe Willem E. Mesenchymal Stromal Cells: Sensors and Switchers of Inflammation. *Cell Stem Cell*. 2013;13(4):392-402.
118. Otero-Viñas M, Falanga V. Mesenchymal Stem Cells in Chronic Wounds: The Spectrum from Basic to Advanced Therapy. *Adv Wound Care (New Rochelle)*. 2016;5(4):149-63.
119. Popov A, Scotchford C, Grant D, Sottile V. Impact of Serum Source on Human Mesenchymal Stem Cell Osteogenic Differentiation in Culture. *International journal of molecular sciences*. 2019;20(20):5051.
120. Birnbaum T, Roider J, Schankin CJ, Padovan CS, Schichor C, Goldbrunner R, et al. Malignant gliomas actively recruit bone marrow stromal cells by secreting angiogenic cytokines. *Journal of Neuro-Oncology*. 2007;83(3):241-7.
121. Sun C, Dai X, Zhao D, Wang H, Rong X, Huang Q, et al. Mesenchymal stem cells promote glioma neovascularization in vivo by fusing with cancer stem cells. *BMC Cancer*. 2019;19(1):1240.
122. Caplan AI. Mesenchymal Stem Cells: Time to Change the Name! *STEM CELLS Translational Medicine*. 2017;6(6):1445-51.
123. Del Fattore A, Luciano R, Saracino R, Battafarano G, Rizzo C, Pascucci L, et al. Differential effects of extracellular vesicles secreted by mesenchymal stem cells from different sources on glioblastoma cells. *Expert Opinion on Biological Therapy*. 2015;15(4):495-504.
124. Figueroa J, Phillips LM, Shahar T, Hossain A, Gumin J, Kim H, et al. Exosomes from Glioma-Associated Mesenchymal Stem Cells Increase the Tumorigenicity of Glioma Stem-like Cells via Transfer of miR-1587. *Cancer Research*. 2017;77(21):5808-19.

125. Ma Z, Cui X, Lu L, Chen G, Yang Y, Hu Y, et al. Exosomes from glioma cells induce a tumor-like phenotype in mesenchymal stem cells by activating glycolysis. *Stem Cell Research & Therapy*. 2019;10(1):60.
126. Dührsen L, Hartfuß S, Hirsch D, Geiger S, Maire CL, Sedlacik J, et al. Preclinical analysis of human mesenchymal stem cells: tumor tropism and therapeutic efficiency of local HSV-TK suicide gene therapy in glioblastoma. *Oncotarget*. 2019;10(58):6049-61.
127. Pacioni S, D'Alessandris QG, Giannetti S, Morgante L, De Pascalis I, Coccè V, et al. Mesenchymal stromal cells loaded with paclitaxel induce cytotoxic damage in glioblastoma brain xenografts. *Stem Cell Research & Therapy*. 2015;6(1):194.
128. Yong RL, Shinojima N, Fueyo J, Gumin J, Vecil GG, Marini FC, et al. Human Bone Marrow-Derived Mesenchymal Stem Cells for Intravascular Delivery of Oncolytic Adenovirus  $\Delta$ 24-RGD to Human Gliomas. *Cancer Research*. 2009;69(23):8932-40.
129. Lang FM, Hossain A, Gumin J, Momin EN, Shimizu Y, Ledbetter D, et al. Mesenchymal stem cells as natural biofactories for exosomes carrying miR-124a in the treatment of gliomas. *Neuro Oncol*. 2017;20(3):380-90.
130. Sharif S, Ghahremani MH, Soleimani M. Delivery of Exogenous miR-124 to Glioblastoma Multiform Cells by Wharton's Jelly Mesenchymal Stem Cells Decreases Cell Proliferation and Migration, and Confers Chemosensitivity. *Stem Cell Reviews and Reports*. 2018;14(2):236-46.
131. Lee HK, Finniss S, Cazacu S, Bucris E, Ziv-Av A, Xiang C, et al. Mesenchymal stem cells deliver synthetic microRNA mimics to glioma cells and glioma stem cells and inhibit their cell migration and self-renewal. *Oncotarget*. 2013;4(2):346-61.

## **Acknowledgment**

This research was made possible by the neurosurgical department of the Klinikum der Universität München. First of all, I would like to thank Prof. Dr. nat. Rainer Glaß and Dr. nat. Roland Kälin for giving me the opportunity to perform scientific studies under their supervision. During my time in the laboratory, they were always willing to help or to discuss my current progress. I wish to acknowledge Prof. Dr. nat. André Brändli and Prof. Dr. med. Rainer Hauck who were part of my mentoring committee. Furthermore, I would like to thank the following people for their support, without whose help this work would never have been possible: Huabin Zhang, Grace Cheng, Enio Barci, Dongxu Zhao, Stefanie Lange and Dorian Kern. I also thank Prof. Dr. Nelson and the group of Prof. Dr. Spitzweg for their ongoing collaboration with our department in our experimental work with mesenchymal stem cells. Last but not least I am particularly grateful to my wife and my family who supported me throughout the entire work. I am aware of the fact that I definitely find myself in a privileged situation and not everyone has the same opportunities that I was given. In the end it was my parents who facilitated my education and thereby my future.

# Affidavit



Waechter, Robin

\_\_\_\_\_  
Name, Vorname

Ich erkläre hiermit an Eides statt, dass ich die vorliegende Dissertation mit dem Titel:

***Locoregional heterogeneity of glioblastoma entails pro- or antitumorigenic effects of tumor associated mesenchymal stem cells***

selbständig verfasst, mich außer der angegebenen keiner weiteren Hilfsmittel bedient und alle Erkenntnisse, die aus dem Schrifttum ganz oder annähernd übernommen sind, als solche kenntlich gemacht und nach ihrer Herkunft unter Bezeichnung der Fundstelle einzeln nachgewiesen habe.

Ich erkläre des Weiteren, dass die hier vorgelegte Dissertation nicht in gleicher oder in ähnlicher Form bei einer anderen Stelle zur Erlangung eines akademischen Grades eingereicht wurde.

München, 21.02.2023

\_\_\_\_\_  
Ort, Datum

Robin Waechter

\_\_\_\_\_  
Unterschrift Doktorandin bzw. Doktorand